Development of Environmentally Friendly Chemical Sensor for Detection of Cyanide in Water

Doe-Puplampu Seth

A Thesis Submitted in Partial Fulfillment of the Requirements for the Degree of Master of Science in Environmental Management and Technology (International Program)

Prince of Songkla University

2017

Thesis Title	Development of Environmentally Friendly Chemical Sensor for the Detection of Cyanide in Water.
Author	Mr. Doe-Puplampu Seth
Major Program	Environmental Management and Technology (International Program)

Major Advisor

.....

(Asst. Prof. Dr. Worawit Wongniramaikul)

Co-advisor

.....

(Assoc. Prof. Dr. Aree Choodum)

Examining Committee:

.....Chairperson

(Dr. Wilasinee Sriprom)

.....Committee

(Asst. Prof. Dr. Worawit Wongniramaikul)

.....Committee

(Assoc. Prof. Dr. Aree Choodum)

.....Committee

(Dr. Supaporn Dawan)

The Graduate School, Prince of Songkla University, has approved this thesis as fulfillment of the requirements for the Master of Science Degree in Environmental Management and Technology.

.....

(Assoc. Prof. Dr. Damrongsak Faroongsarng)

Dean of Graduate School

This is to certify that the work here submitted is the result of the candidate's own investigations. Due acknowledgement has been made of any assistance recieved.

.....Signature
(Asst. Prof. Dr. Worawit Wongniramaikul)
Major Advisor

.....Signature
(Mr. Doe-Puplampu Seth)
Candidate

I hereby certify that this work has not been accepted in substance for any other degree, and is not being currently submitted in candidature for any degree.

.....Signature

(Mr. Doe-Puplampu Seth)

Candiddate

Thesis Title	Development of Environmentally Friendly Chemical Sensor for Detection of Cyanide in Water
Author	Mr. Doe-Puplampu Seth
Major Program	Environmental Management and Technology (International Program)
Academic	2017

Abstract

A rapid quantitative colorimetric determination of CN^- was developed by synthesizing BF_2-curcumin reagent. Borontriflouride was added to the carbonyl group of curcumin, an extract from turmeric. Parameters affecting to the synthesis and reaction products were optimized. The optimum parameters were found to be 1 mM BF_2-curcumin concentration, sample pH of 9 and 5 minutes reaction time. The reagent was synthesized within a micro tube to which the sample can easily and directly be added for an in-tube detection. The reaction mechanism with cyanide relied on the deprotonation of the hydroxyl group of BF_2-curcumin. The orange-red color of BF_2-curcumin solution changed to blue upon reaction with cyanide solution. Tapioca flour was used as polymeric material in which the reagent was embedded. Parameters affecting to the synthesis of the BF_2-curcumin synthesized starch film were also optimized. An innovative free of charge application installed on a mobile phone was used to capture and measure the color intensity of the reaction product. A digital image analysis was applied to the reaction product to obtain analytical data in the form of Red Green Blue (RGB) values. Quantification was achieved by exploiting the relationship between RGB value and concentration of colorimetric product. A considerably lower detection limit (0.12 ± 0.007) and (0.40 ± 0.021) were obtained for the reagent and sensor analysis respectively. An efficient linear range (0.2 – 7 mg/L) and good sensitivity were achieved. The method validation point out good intra- and inter-day precision for both the reagent and the synthesized starch film. Accuracy of the developed method was excellent in analytical

performances. Water sample from an abandoned tin mine site were analyzed using the sensor and the results were in good agreement with spectrophotometer analysis.

Keywords: Cyanide, mobile phone, RGB Color system, curcumin, colorimetry.

Acknowledgement

First and foremost, I would like to thank the Almighty God for seeing me through this study. I would like to show my profound gratitude to my advisors, Asst. Prof. Dr. Worawit Wongniramaikul and Assoc. Prof. Dr. Aree Choodum – On for their guidance, advice, encouragement and motivation. Their doors were always open whenever I ran into a trouble spot or had a question about my research or writing. Their efforts are deeply appreciated and I am happy to have them through this study. Besides my advisors, I would like to thank the rest of my thesis committee: Dr. Wilasinee Sriprom and Dr. Supaporn Dawan for their insightful comments.

I would like to also express my sincere gratitude to the Faculty of Environmental Management Technology, Prince of Songkla University (Phuket Campus) for giving me the opportunity to enhance my knowledge through this program and also the scholarship for the study.

I am grateful to Applied Chemistry and Environmental Technology Research Centre (ACET-RC) headed by Assoc. Prof. Dr. Aree Choodum for offering me scholarship and also the opportunity to be part of their research group.

Finally, I would like to thank my parents, Mr. Doe-Puplampu and Mrs. Grace Doe not forgetting my amazing sisters Salomey and Elizabeth. Their help and support throughout my educational life will never be forgotten. This accomplishment would not have been possible without them. God richly bless them all.

Doe-Puplampu Seth

Contents

Content (cont.)

Content (cont.)

Content (cont.)

List of Table

List of Figures

List of Figures (conti.)

List of Abbreviation

LED	=	Light Emitting Diode
PCR	=	Polymerase Chain Reaction
RGB	=	Red Green Blue
RSD	=	Relative Standard Deviation
SEM	=	Scanning Electron Microscopy

CHAPETER 1

Introduction

1.1 Background/ Problem statement

The exponential increase in industrial activities over the past few decades has contributed to the release of several hazardous pollutants such as F^-, S^{2-}, HSO_4^-, CN^- and $H_2PO_4^-$ into the atmosphere and aquatic ecosystem (Persuad, 1982). Cyanide anion is inevitably one of the most abundant and poisonous anion which in a very small concentration can be lethal to humans and almost all other forms of life (Selkoe, *et al*., 2003).

In spite of its extreme toxicity, cyanide is produced in large quantities for its important role in several industrial activities such as electroplating, metallurgy, gold mining and synthesis of fabric and plastics (Kulig, *et al*., 1991; Miller, *et al*., 2001 and Baud, *et al*., 2007). Other cyanide sources include vehicle exhaust, burning of municipal waste, and the use of cyanide-containing pesticides. Cyanide in landfills is another source which can contaminate underground water. It is also present in the air when a building is burning usually because of cyanide-containing plastics. In air, cyanide is present mainly as gaseous hydrogen cyanide. Some amount of cyanide in air is present as fine dust particles. The dust eventually settles over water. Water is therefore a major of been exposed to cyanide. Despite the increasing level of monitoring and strict control, accidental releases of cyanide into the environment do occur and presents great danger to the environment. The disastrous spill of millions of liters of cyanide waste in Romania in 2000 is considered as the worst case of water pollution in Europe ever (Koenig, *et al*., 2000).

Cyanide has several means of getting into the body which includes the digestive tract, respiratory tract, skin and other ways, causing vomiting, cramps, loss of consciousness and to a larger extent death (Zheng, *et al*., 2011). Moreover, it also has the ability to affect several functions of the human health, including the visual, vascular, endocrine, central nervous and metabolic systems (Martinez, *et al*., 2006 and Gale, *et al*., 2015).

Another major problem associated with cyanide release in the environment is that, fish and aquatic invertebrate are usually sensitive to its exposure. Concentration of free cyanide in the aquatic environment ranging from 5.0 to 7.2 micrograms per liter reduces swimming performance and also inhibit production in many species of fish. Concentrations of 20 to 72 micrograms per liter free cyanide causes the death of many species, and concentration in excess of 200 micrograms per liter are rapidly toxic to most species of fish. Invertebrate experience adverse nonlethal effects at 18 to 43 micrograms per liter of cyanide and lethal effect at 30 to 100 micrograms per liter (Eisler, *et al*., 1999). Cyanide anion is therefore regulated because of its potential significant impact not only on human health but also the environment.

The World Health Organization (WHO) has set 1.9 μM as the maximum permissive level of cyanide in drinking water due to its formidable toxicity (Kaur, *et al*., 2012). In addition to WHO, it is regulated as an environmental contaminant by the United States Environmental Protection Agency (EPA) for drinking water, surface water, and wastewater due to their health concerns. For drinking and surface water, the EPA has established a maximum contamination level of 200 mg/L free cyanide determined by a total cyanide assay. The EPA also specifies 5.2 mg/L total cyanide continuous discharge limits for publicly own treatment works (POTW) and 22 mg/L as maximum discharge into fresh water. For salt water bodies, the continuous and maximum discharges are 1 mg/L total cyanide. The EPA defines these continuous (4d) and maximum (1 h average) limits to ensure that aquatic life is unharmed. (National Primary Drinking Water Regulation 2008 and Water Quality Standards 2008).

The extreme toxicity and wide spread usage of cyanide makes environmental testing critically important. This has led to considerable research into the development of selective and sensitive approach for its detection. A wide range of conventional methods have previously been employed to the quantitative analysis of CN^- in aqueous media (Raju, *et al*., 1989; Kage, *et al*., 1994 and Shan, *et al*., 2004). These conventional methods are ideal for high precision analysis. However, their use require sophisticated instrumentation and long processing time.

Chemical sensor is one attractive analytical tool which has attracted the interest of several researchers in recent times due to their numerous advantages such as portability and cost effectiveness over the traditional methods. Chemical sensors enable on-line and field monitoring and therefore can be a useful alternative to the conventional approach. The field of chromogenic and fluorogenic chemosensors among other chemical sensors for CN^- detection in water has also experienced a rapid growth in recent years (Chen, *et al*., 2010; Lee, *et al*., 2010; Jung, *et al*., 2011; Buske, *et al*., 2015; Nicoleti, *et al*., 2015, and Pati, *et al*., 2016). The apparent reason for cyanide detection through chromogenic colorimetry is to design an easy and portable detection kit. Change in color of the reaction product which can be observed with the naked eye makes implementation of this techniques practicable in rural and urban areas. For this purpose of chromogenic colorimetry, various materials have been reported in fabricating colorimetric sensors (Tomasulo, *et al*., 2005; Xu, *et al*., 2010 and Santos, *et al*., 2014). However, most of these systems need to be carried out in either organic solvents or mixture of organic solvents and water which limits their application to the analyses in aqueous solution. In addition, most of these materials are not readily available which makes obtaining them expensive and sometimes detrimental to the environment. The use polymeric material with chromogenic or/and fluorogenic units embedded in their molecular structure is another system which has attracted much attention due to their specific selectivity (Isaad, *et al*., 2013; Busschaert, *et al*., 2015; Wu, *et al*., 2015 and Sharma, *et al*., 2016(b),).

Spectrophotometric technique is one analytical instrument that has been employed for quantifying colorimetric product in the past few decades (Byrne, *et al*., 2000 and Lopez-Molinero, *et al*., 2010). Inasmuch of the high precision and accuracy associated with this technique, it requires appropriate instrument and skilled persons. In addition, the size of the instrument and operational procedure restricts its usage in the laboratory. In view of this, the development of a rapid, cost effective and simple method to exploit the relationship between concentration of analyte and the colorimetric reaction will be beneficial.

Herein, BF_2-curcumin was synthesized as a simple, rapid and low cost colorimetric reagent for detecting cyanide in water by both naked eye and using digital image analysis. The reaction mechanism of this proposed reagent and cyanide anion was based on the deprotonation of the hydroxyl group of BF_2-curcumin. Curcumin as a choice is due to its natural availability and also its interesting photochemical properties. Due to the advantages associated with the use of polymeric materials with chromogenic units embedded in their molecular structure such as specific selectivity of analyte and their excellent film forming properties. It was therefore of interest to incorporate BF_2-curcumin regent into the molecular structure of starch (tapioca flour). Tapioca flour is known to be an environmentally friendly polymer which is readily available in almost all parts of the world. A free-of-charge application installed on a mobile phone was successfully employed for the colorimetric analysis to obtain analytical data in the form of Red Green Blue (RGB) values. A laboratory-built protective box was used during measurement of the RGB values to limit environmental light interference.

1.2 Research objective

To synthesize and design a simple, inexpensive and an environmentally friendly colorimetric detection kit to detect free cyanide in water without the need for special reaction conditions or sample pre-treatment. This cost effective detection system will be easy to handle and results readily understood.

1.3 Scope

1.3.1 BF_2-curcumin was used as the colorimetric test kit to detect cyanide in water

1.3.2 The test kit is produced in two forms, *i.e*. BF_2-curcumin reagent and polymer sensor (BF_2-curcumin synthesized starch film)

1.3.3 The optimum conditions for synthesis of the reagent were 1 mM BF_2-curcumin concentration, pH 9 of sample and 5 minutes reaction time

1.3.4 The optimum condition for synthesis of polymer sensor were 0.05 g of flour, 5 mM BF_2-curcumin concentration, 60 ^{o}C oven temperature, 90 minutes of time spent in the oven, sample pH of 9, 100 mL of solution in the micro tube and 5 minutes reaction time.

1.3.5 The biopolymer for entrapping the color reagent was made from tapioca

1.3.6 The mobile phone and its application program was applied as the color detector and RGB analyzer respectively.

1.3.7 Analytical performing parameters that were investigated were limit of detection, accuracy, precision and linear dynamic range.

1.3.8 The effect from ion interferences, which were Cl^-, NO_3^-, SO_4^{2-}, and PO_4^{3-} on CN^- were studies in this research.

1.3.9 Water sample from an abandoned mine site was collected and analyzed by the regent and developed sensor, comparing with the standard spectrophotometric method.

1.4 schematic diagram

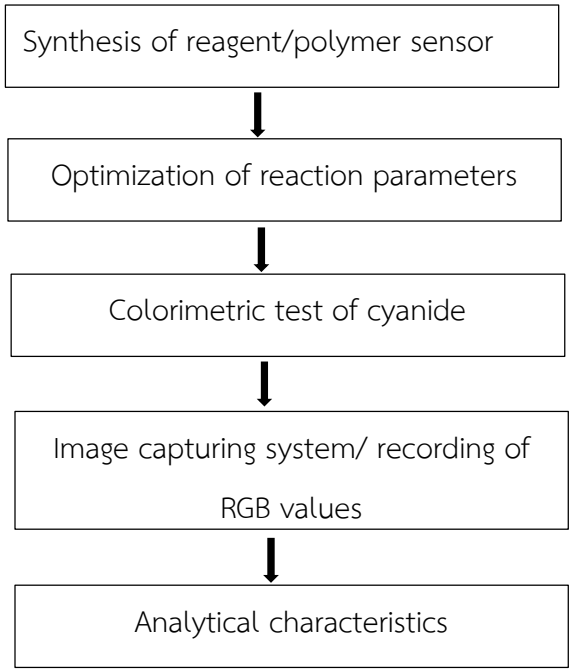

Fig 1.1 Summary of experimental flow chat

CHAPTER 2

Literature Review

2.1 What is cyanide?

Cyanide ion is a simple molecule consisting of one carbon and one nitrogen atom connected together by a triple bond. It carries a negative charge of 1. Cyanides can be produced from both anthropogenic and natural sources. They are naturally found in a number of food and plants such as almonds, spinach, millet sprout and bamboo shoot. They can also be produced by certain bacteria, fungi and algae. Cyanide ion does not exist alone and one common form is the hydrogen cyanide (HCN), which is normally breathed in as gas. One major use of hydrogen cyanide is its application in the production of insecticides for fumigating enclosed spaces. Hydrogen cyanide has also been used in gas chamber executions. The other forms of cyanide compounds which can be mostly found in the environment is potassium and sodium cyanide. Cyanide compounds are mostly released into the environment during the course of industrial activities or from smoke of vehicles. Sodium cyanide which is a white and cubic crystalline is predominantly use in the extraction and recovery of minerals and metals from ores, specifically in the cyanidation of gold and silver. Cyanidation technique for gold recovery is the largest mining use for sodium cyanide. Electroplating, especially of zinc, copper and brass is another area that involves the use of NaCN. Potassium cyanide which is also a white crystalline solid that dissolves to liquid by absorbing moisture from air is also used primarily for fine silver plating and can also be used for dyes and specialty products (Jenk, 1985).

In air, cyanide is present mainly as gaseous hydrogen cyanide. Some amount of cyanide in air is present as fine dust particles. The dust eventually settles over water. Water is therefore a major of been exposed to cyanide. The major sources of cyanide in water are discharges from some mining processes, electroplating and organic chemical industries. Humans are exposed to cyanide mostly by drinking cyanide contaminated water. Breathing smoke-filled air during fires may also be a source of cyanide exposure.

2.2 Health hazards of cyanide

The toxicity of individual cyanide compounds is dependent on the concentration of which one consumes. Cyanide is well known acute toxins that exerts its primary toxicological effect by binding to the metallic cofactor metalloenzymes, thereby preventing enzymes and cell functions. This occurrence prevents cellular respiration by irreversibly binding the iron in cytochrome C oxidase. In addition, thiocyanate which is metabolized from cyanide, interferes with iodine uptake by the thyroid gland, causing goiters and other long-term iodine deficiency diseases (Vennesland, 1981; Noh, *et al*., 2003, Simeonoya, *et al*., 2004 and Na, *et al*., 2014). After decomposition of cyanide in the human body, it affects the body's multiple organs and tissues, including blood circulation, vision, central nervous system, endocrine system and digestive system.

2.3 Conventional approach for CN^- detection

Accurate detection of cyanide has become increasingly important to the regulated agencies and the general public due to its extreme toxicity. Standard methods such as titrimetric, colorimetric and cyanide-selection method have been reported as standards to quantify cyanide anions. These methods are ideal for high accuracy and precision. However, their applications requires expensive chemicals and instrument for sample treatment. In addition, their applications are time consuming and also requires experts. Other various conventional methods such as electrochemical, chromatography, potentiometric and voltammetric have previously been employed for the detection of CN^- in aqueous media. These methods are also ideal for high precision and accuracy. However, these analytical techniques requires instrument that are expensive. Furthermore, these instruments are bulky which makes them suitable for use only in the laboratory. In view of this, samples have to always be collected on site and conveyed to the laboratory for analysis. Contamination and loss of samples may occur during transportation. Other drawbacks are either the laborious multistep sample treatment, the use of special reaction conditions as well as the low tolerance towards the presence of other anions. However, in the last years smaller, portable and less expensive devices have been brought to the market.

Electrochemical detection by direct current (DC) amperometric or pulsed amperometric detection (PAD), is sensitive and selective electrochemical approach which is suitable for direct determinations of cyanide anions. However, PAD is preferred over DC amperometry. This is because the working electrode in PAD is cycled through three or four voltage potentials every second. This process results in an electrode surface which is continually cleaned, whereas in DC amperometry, the working electrode can foul over time, leading to a loss in peak response (Weinberg, *et al*., 2002). Even though electrochemical detection of CN^- proved to have good sensitivity and selectivity, it however requires extensive and time consuming procedures.

Ion-Exclusion chromatography with Pulsed Amperometric Detection for total cyanide is another conventional area that has been reported. In this method, the advantages of ion exchange with the sensitivity, selectivity, and stability of pulse amperometric detection using a Pt working electrode were combine to directly detect cyanide without any interferences from chloride and sulfide (Christison, 2015). On the contrast, this method involves complex system preparation leading to the development of other techniques such as the optical chemical sensors.

2.4 Optical chemical sensors

Over the last few decades, the synthesis and design of optical chemosensors for the detection of anion especially CN^- have received extensive attention. This is because of their simplicity, cost effectiveness and also their ability to be used on site. The optical properties measured can be absorbance, fluorescence and reflectance. Most optical chemical sensors are composed of a recognition component and a transduction component. The transduction component is responsible for accepting signal from the recognition component and converting it to a signal that can be analyzed. The process of chemical recognition can be achieved by oxidation-reduction or by chemical binding/non-binding interactions. Different light source have been reported in the application of optical sensors. Light emitting diodes (LEDs) have recently been used as a light source for optical sensor. LEDs have shown great potential to perform optical measurements within microfluidic sensing devices by providing high brightness and high efficiency that can investigate small sample volumes and low analyte concentrations. Many research have explored the use of LED as a source of light to produce inexpensive and low power detectors for incorporating colorimetric methods into remotely deployed systems (Bui, *et al*., 2015).

Optical sensors, in which a change in color and/or fluorescence intensity is monitored is another analytical area which has attracted the interest of several scholars in the past few years. They exhibit many advantages such as rapid implementation, large dynamic range and multiplexing capabilities over the conventional method. In addition, optical chemical sensors can provide simple and convenient procedures for on-site analysis. Such sensors are extremely user friendly in the sense that they can be operated even by less skilled personnel and does not require extensive calibrations.

A simple and inexpensive optical absorption one-shot sensor membrane for cyanide detection in water was reported by Chamjangali, *et al*. in 2001. The chemical sensor was constructed by immobilizing crystal violet (CV) on triacetylcellulose membrane. These sensors are self-contained analytical devices with reagents incorporated in a dry format that respond semi-quantitatively or quantitatively to the CN^-. The working principle of the sensor was basically by the reaction between cyanide anion and the immobilized CV at pH=5.4. This leads to a decrease in absorbance of the membrane at 600 nm. The response of the sensor was therefore recorded by measuring the decrease in the absorbance of CV at 600 nm. The sensor showed several advantages such as low cost, easy fabrication and also good mechanical properties. However, preparation of sensing membrane proved to be time consuming and also the entire reaction used special conditions.

2.4.1 Fluorescence-based optical chemical sensor

Fluorescence-based optical sensor has seen a remarkable growth in various fields of modern sciences such as biochemistry, biotechnology, clinical diagnostic and environmental sciences. Compared to the conventional methods, fluorescence based chemical sensors distinguish itself to be a good transduction mechanisms to report chemical recognition (Lakowiez, 1991). Fluorescence-based detection which normally depends on the intensity change at a single wavelength has also been reported as an optical chemical sensor and has attracted much attention over absorption spectroscopy.

This is due to its high sensitivity and easy implementation under diversified environmental conditions (Chen, *et al*., 2015).

Peng, *et al*., (2009) reported about a fluorescence turn-on sensing ensemble of cyanide with a trifluoroacetylamina group in aqueous media solution by making use of the aggregation-induced-emission (AIE) feature of silole compounds. The turn-on output fluorescence signal of fluoresecence probe is more advantageous than the turn-off response. The apparent reason is that, the turn-on output signal is able to appreciably elevate the signal-noise ratio and make the fluorescence visualization easier to be realized. Even though silole derivatives are reported to be weak fluorescent in solution but becomes highly fluorescent after aggregation. This fascinating phenomenon was referred to as aggregation induced enhanced emission (AIE) first reported by Luo, *et al*. in 2001. They reported that the ensemble displayed good selectivity towards cyanide over other common inorganic anions. Several reports of chemosensors have been made on the basis of the AIE feature of silole and relevant compounds (Tong, *et al*., 2007, Yuning, *et al*., 2009). In spite of the high selectivity and sensitivity of fluorescence probe technique, the signal output could easily be influenced by factors such as environmental conditions, probe distribution and instrumental efficiency (Komatsu, *et al*., 2007, Srikum, *et al*., 2008). To overcome this shortcoming, ratiometric fluorescence sensing has been employed and this allows the measurement of relative emission intensities at different wavelengths. This can serve as an internal reference for self-corrected and hence the reliability of the measurements is significantly enhanced (Tremblay, 2007).

Ratiometric response means the fluorescence changes at two different wavelengths simultaneously. This two-channel fluorescence response usually offers high signal-to-noise ratio (S/N) and it is very helpful intercellular measurements. This is because, it can eliminate most fluorescence change caused by the effects which are not related to the analytes of interest.

In 2015, Kew-Yu, *et al*., proposed a structurally simple 7-azaindole-based chemodosimeter for the first time as a ratiometric fluorescent probe. The probe was able to sense CN^- with specific selectivity in aqueous media. The mechanism of the

sensor was based on excited-state intermolecular charge transfer (Zhang, *et al*., 2013). In their method, a decrease of the absorption band from 362 nm to 293 nm shows the presence of CN^-. Their method showed good selectivity and allowed the measurement of relative emission intensities at two different wavelengths, which can serve as an internal reference for self-correction.

Long *et al*., (2013) also designed a compound as a novel fluorescence ratiometric probe for cyanide detection in aqueous media. A solution of acetophenone and pyrroldine in $CHCL_3$ was synthesized to develop the compound. Upon treatment with CN^-, the fluorescence of the probe exhibited red shift from 570 nm to 608 nm which shows a good selective responds towards cyanide. Ratiometric fluorescence based sensor turns to compliment the drawbacks of a normal fluorescence base sensor. However this method showed to be time consuming because of the multistep sample preparation.

2.4.2 Fluorescence and colorimetric based optical chemical sensors

Because of its rapid implementation and unambiguous response in aqueous media, colorimetric fluorescence based sensors have also been reported in recent years. Most recently Jun-Jian *et al*., 2016 designed a naphthalene-malononitrile compound as a colorimetric fluorescence sensor towards cyanide. The designed focused on the utilization of nucleophilic addition reaction of CN^- with dicyano-vinyl group of the sensor. Upon the addition of CN^-, the sensor displayed very large blue-shift in both fluorescence (80 nm) and absorption (120 nm) spectra. The sensor which showed a good sensitivity, selectivity and fast response to CN^- was synthesized by 2-((6-(dimethylamino) naphthalene-2-yl) methylene) malononitrile. The electron-withdrawing nature of the dicyano-vinyl group of the sensor gave it a very high sensitivity and selectivity to CN^-.

A donor-two acceptor sensor where a novel-base fluorescence and colorimetric sensor was design and synthesized based on 3-ethyl-2-methyl-1-2-methyl-1, 3-benzothiazol-3-ium iodide and 5-nitrosalicyclaldehyde has also been reported. The benzothiazol site of the sensor was an effective target for the nucleophilic analytes. A visible color change from red to faint yellow as well as fluorescence turn-on response is

observed when cyanide ion was added to the solution of the sensor. Other anions could not interfere with the cyanide detection and also the method gave a very good detection limit (Junjian, *et al*., 2015). Inasmuch as fluorescence and colorimetric sensor demonstrated to have a very quick respond to cyanide, good selectivity and sensitivity, most of the reports on them involved the use of sophisticated instrument for sample preparation and quantification.

Shan, *et al*., (2013) reported on the derivatives of two bromine substituted indole chalcone as a colorimetric fluorescence chemosensors for cyanide. The reagents were synthesized by way of typical condensation between 2-(hydroxyl)-4-bromine acetophenone and 3-indolealdehyde or N-ethyl-3-indolealdehyde. They concluded that the compounds exhibited quick and obvious color fluorescence turn-on charges to cyanide and with color changes from yellow to red or from light yellow to deep yellow. However, their results showed to respond effectively in only acetonitrile solution and hence there has to be always sample treatment.

To the degree that, fluoresecence based optical sensors are good alternative to the conventional approach of cyanide detection, some natural products with intrinsic fluorescence turns to inhibit the accuracy of the technique.

2.4.3 Colorimetric based sensors

The use of colorimetric sensor in environmental analysis especially in the area of cyanide detection has attracted considerable attention. This technique can give simple visual results for “naked-eye” detection. Colorimetric sensors as the name would suggest, are based upon detection of an analyte-induced color change in the sensor material.

Liu, *et al*., (2012) synthesized a new reagent for detecting CN^- which based on the absorbance of the reaction to obtain the optical signal. The new reagent which produced a color change from colorless to yellow when encountering cyanide was developed by the synthesis of 2-amino-10-ethyl-acridone. Trifluoroacetic acid groups was added to the reagent to improve its optical properties. As this method showed to be

simple and also gave a quicker determination results, it however revealed poor ability of anti-interference. Other interference ion such as F^-, Cl^-, Br^- and I^- showed a faint yellow color which was not far from the yellow color showed by the cyanide ions.

Bhowmick, *et al*., (2016) reported on metallic-based coordination complexes for cyanide detection. They investigated Co^{II} bis (terpyridine) complexes as instant naked eye colorimetric detectors of cyanide anions in micromolar concentration in polar solvents, including water following the formation of the corresponding Co^{III} trycyanide complex. They used UV-vis spectroscopic method to monitor the quantitative detection of cyanide.

Considering the several advantages associated with colorimetric method of cyanide detection, many of the anion sensor are not capable of distinguishing cyanide effectively from other anions such as F^- and OAc^-. The obvious reason is that, these anions possess similar basicity to CN^- and easily form hydrogen bonds. In order to overcome such limitation, Jo, et al., (2015) synthesized a colorimetric chemosensor by condensing hydrazine with 3.5-dichloro-2-hydroxybenzaldehyde which could distinguish cyanide effectively from anions such as F^- and OAc^-. The sensor could detect cyanide by color change from colorless to yellow via the "naked-eye" in aqueous media. Although their sensor showed good selectivity of cyanide among other anions, quantification and monitoring of the CN^- required the use of expensive and sophisticated instrument. (Hyun, *et al*., 2015).

Chaicham, *et al*., (2010) synthesized and investigated the photophysical and photochemical properties of derivatives of BF_2-curcumin. The derivatives of difluoroboron curcumin exhibited different optical properties depending on the substituents on the benzene rings. A cyanide sensor with good selectivity and sensitivity was obtained upon the addition of BF_2 on the curcumin structure. Addition of BF_2 to the carbonyl group of the curcumin improved the photophysical properties and stability of the curcumin by inhibiting the keto-enol tautomerization. BF_2-curcumin gave a very good chemical sensor for cyanide detection by the naked eye over the other derivatives. The method proved to be fast, convenient and also could be carried out in an aqueous

solution, however for a good detection limit and a better resolution a spectrophotometry was required.

2.5 Polymeric material

Due to the advantages associated with the use of polymeric materials with chromogenic units embedded in their molecular structure such as specific selectivity, simple process ability and also excellent film forming properties (Eggins, 2002). It was of interest to embed BF_2-curcumin reagent into the molecular structure of tapioca flour. In addition, polymers are convenient due to their simple process ability to small particles and thin film which can be deposited onto optical fibers for sensor fabrication. It was therefore of interest to incorporate BF_2-curcumin regent into the molecular structure of a polymer. Starch (flour) is one of the most abundant naturally polysaccharides. There is renewed interest in the starch-based materials in recent years in other to exploit its biodegradability properties. Starch is mainly composed of two homopolymers of D-glucose, amylose and amylopectin. Amylose is almost a linear polymer with a-D-(1/4) glycosidic linkages, while amylopectin is a highly branched polymer which contains a-D-(1/6) glycosidic linkages at the branching points in addition to a-D-(1/4) glycosidic linkages (Cura, *et al*., 1995).

Isaad, *et al*., (2013) presented about the preparation and characterization of the biosourced plastic film starting from starch as a biopolymer. The polymer was charged by a chromogenic probe based on quinolinium merocyannine derivative for cyanide anion detection in pure water. They revealed the final functionalized starch film to aqueous solutions of various anions to investigate its selectivity and sensitivity towards cyanide. They prepared the starch film by dispersing 5 g of starch in water-glycerol solution. They added HCl solution and dye after which they heated the mixture on a hot plate to obtain a clear solution. Sodium hydroxide solution was

subsequently added and the resulting starch solution was then poured onto a Teflon-coated glass plates. The cast starch films were allowed to air dry for about 48 hours before peeling. They incorporated the organic chemodosimeter into the starch film. Their study indicated that the film only changed color from yellow to purple in the presence of cyanide. Their easy-to-use material showed a high degree of cyanide selectivity in aqueous medium. However, the preparation of the required several processes.

Curcumin and starch (tapioca flour) as a choice of materials was basically due to their natural availability and low cost. BF_3-curcumin reagent was synthesis and embed in the molecular structure of a polymer.

2.6 Turmeric

The turmeric (curcuma longa) plant, a perennial herb belonging to the ginger family, is cultivated extensively in south and southeast tropical Asia. The rhizome of this plant is also referred to as the "root" and it is used as a dietary spice, coloring agent in foods and textile. It is also use as treatment for a wide variety of ailments. It is widely used in traditional Indian medicine to cure biliary disorders, anorexia, cough, diabetic wounds, rheumatism, and sinusitis. Turmeric paste in slaked lime is a popular home remedy for the treatment of inflammation and wounds. The most active component of turmeric is curcumin, which makes up 2 to 5 percent of the spice. Curcumin consist of two methoxy phenols conjugate through alpha, betta-unsaturated betta-diketone linker, which can perform a keto-enol tautomerism. A few investigations concerning photophysical properties of curcumin for medicinal chemistry have been reported (Aggarwal, *et al*., 2006).

The characteristic yellow color of turmeric is due to the curcuminoids, first isolated by Vogel in 1842. Curcumin is an orange-yellow crystalline powder practically insoluble in water (Bagchi, *et al*., 2012). For centuries, curcumin has been consumed as a

dietary spice at doses up to 100 mg/d. Extensive investigation over the last five decades has indicated that curcumin reduces blood cholesterol. (Aggarwal, *et al*., 2006).

Curcumin surprisingly exhibits many interesting photophysical and photochemical properties. The absorption band is approximately 408 - 560 nm in most organic solvents while fluorescence spectrum is solvent-sensitive with emission wavelength from 460 - 560 nm (Barik, *et al*., 2003). Currently, boron difluoride-containing molecules represent a topical class of fluorophores that encompasses a broad variety of chemical structures such as anils, 2-benzoxazole, with boron-dipyrromethene derivatives representing the most dyes. These materials display outstanding electronic and optical properties (Mattew, *et al*., 2016).

As mentioned above, curcumin was used to produce the chemical reagent which was subsequently anchored into a polymer to design an environmentally chemosensor to detect cyanide ion in water. The developed method involved the use of mobile a phone as an analytical device. Mobile phone as a choice of analytical instrument is basically due to its portability and its ability to be deployed as a rapid field test device. Mobile phones have become pervasive in society and are typically equipped with a high resolution digital camera which can be used to produce an image expediently. The colored product from the reaction of cyanide and the sensor was quantified using a free of charge application of photography where the relationships between Red Green Blue (RGB) values and the concentrations of the colorimetric product were exploited.

2.7 Colorimetric quantification

Quantification of colorimetric product by spectrophotometric technique is one analytical area that has received much attention in the past few decades (Lou *et al*., 2009, PitschmannV, 2011; Tivana, *et al*., 2014). Spectrophotometric technique exhibit several advantages such as high precision and accuracy, however, its application

requires appropriate instrumentation and skilled person. In addition, the size of the instrument and operational procedure restricts its usage in the laboratory. It also requires several steps of sample preparation which makes the entire process time consuming. In view of this, the development of a rapid, cost effective and simple method to exploit the relationship between concentration of analyte and colorimetric reaction will be beneficial.

Several reports have been made by researchers on the use of digital imaging for colorimetric quantification testing. Digital image-based analysis evaluates the RGB data obtained from digital image of a reaction product. The use of mobile phone or digital camera to capture the image of a reaction product for colorimetric analysis of various chemicals has been highlighted and reported by several researchers (Epperson, *et al*., 1998; Gaiao, *et al*., 2006; Lopez-Molinero, *et al*., 2010; Caciano de Sena, *et al*., 2011; Choodum, *et al*., 2011, Choodum, *et al*., 2012 and Choodum, *et al*., 2014). The captured digital image is generated by means of the light reflection from targeted color species through three different filters, red (R), green (G) and blue (B). Results are obtained as individual RGB values, and the final color is composed from the additive data of the three RGB filters. The evaluation of Red Green Blue (RGB) value of the reaction product captured on the digital image could be used to indicate the concentration of pollutants in samples. Thus colorimetric reaction integrated with digital image analytical technique fulfills quantitative performance of the developed sensors (Suzuki et al., 2006). With this process the cyanide measurement can be performed at the field and not necessarily carrying samples to the laboratory.

Obtaining analytical data in the form of RGB values from the captured image is basically by virtue of digital image received from a standard trichromatic response of a particular image. The RGB intensity data produces values ranging from 0 to 255 for each channel (Byrne, *et al*., 2000, Gaiao, *et al*., 2006). That is, a black digital image will produce an R, G, B value of 0, 0, and 0 respectively, whereas a white digital image will produce R, G, B value of 0, 0, and 0 respectively. This phenomenon agrees with the fact that a black digital image absorbs all the light rays without any form of light reflectance whiles a white digital image reflects all light rays which are directed towards it. In addition,

the colors obtained from each of the three channels are subtractive colors and selectively absorb certain wavelength of light, thus affecting the observed eye.

Several innovative application such as Matlab image processing tool box (Goddijn, *et al*., 2006, Lopez-Molinero, *et al*., 2010,) and Adobe Photoshop (Choodum, *et al*., 2011) have been reported to obtained analytical data in the form of RGB from a digital image for the quantification of a specific analyte. These quantification approach are based on the measurement of the shades of colorimetric products in digital image of the test. In spite of the fact that color is intuitive, the use of color spaces and imaging devices facilitate the use of color for quantification (Cantrell, *et al*., 2009)

With regards to using digital camera images, processed in Adobe Photoshop, Thongprajukaew, *et al*., (2014) also reported on the colorimetric determination of amylase activities. They used iPhone imaging and Adobe Photoshop image analysis to obtain and analyze intensities and absorbance of red, green and blue (RGB) values. Their approach in quantifying amylase specific activity from commercial source compared with that of spectrophotometric measurement were not significant.

Choodum, *et al*., (2013) reported on the use of iPhone as a device for rapid quantitative analysis of trinitrotoluene in soil. Their choice of analytical instrument (iPhone) was to facilitate the development of portable rapid quantitative chemical analysis system as readily available portable device. In their report the built-in camera of a smart phone (iPhone) was used to capture the results from a rapid quantitative colorimetric test for trinitrotoluene (TNT) in soil. They quantified the color of the reaction product using an innovative application of photography where the relationships between the Red Green Blue (RGB) values and the concentrations of colorimetric product were exploited. Their results were comparable with those from spectrophotometric quantification methods. In addition, their results demonstrated that iPhone provides the potential to be used as an analytical instrument.

CHAPTER 3

Methodology

The experiments in this study were separated into 3 parts: synthesis of BF_2-curcumin reagent and polymer sensor, investigation into the analytical performances of the reagent and sensor, application with real sample by the test kits and by standard spectrophotometer method. The results obtained from the real sample analysis by the test kits were compared to that of the standard spectrophotometer method.

3.1 Apparatus

a) Sonicater (S 100 H, Elmasonic, Germany)
b) Evaporator
c) Electrical balance (PA 2102, Ohaus, USA)
d) pH meter (Portable pH/mv Meter, Bante 220, China)
e) Oven (FED 400-UL, Binder, Germany)
f) Hot plate (C-MAG HS 7, IKA, USA)
g) Clinical syringe (Disposable syringe (3 ml), Nipro, Thailand)
h) LED bulbs
i) Protective box

3.1.1 Chemical agents: All analytical grade of chemicals and solvents were obtained from commercial sources (Merck, Aldrich and Burdick & Jackson). The standard cyanide solution was purchased from Fluka (Switzerland).

a) Boron trifluoride diethyl etherate (BF_3, Sigma Aldrich, USA)
b) Ethanol (C_2H_6O 98%, Merck, Germany)
c) Methanol (CH_4O, Merck, Germany)
d) Acetone (C_3H_6O, Burdick & Jackson, Korea)
e) Sodium hydroxide (NaOH 99%, Merck)
f) Hydrochloric acid (HCl 37%, Merck)
g) Chloramine-T trihydrate ($C_7H_7ClNN_aO_2S$, Sigma Aldrich, China)
h) Barbituric acid (Sigma Aldrich, China)
i) Pyridine (Honeywell, Germany).
j) Deionized water
k) Acetic Acid Glacial (CH_3COOH, QRec, New Zealand)
l) Turmeric: Fine powdered turmeric was obtained from a local market in Phuket-Thailand
m) Tapioca flour: Tapioca flour used as a polymeric material was also obtained from a local market in Phuket-Thailand.

3.1.2 Analytical instrument

a) Mobile phone (iPhone 5s). A free of charge application program (Color Assist) was installed on the mobile phone for the colorimetric analysis.
b) Spectrophotometer (HALO RB-10, Dynamica, USA)

3.1.3 Experimental procedure

The experimental procedure is presented as follows:

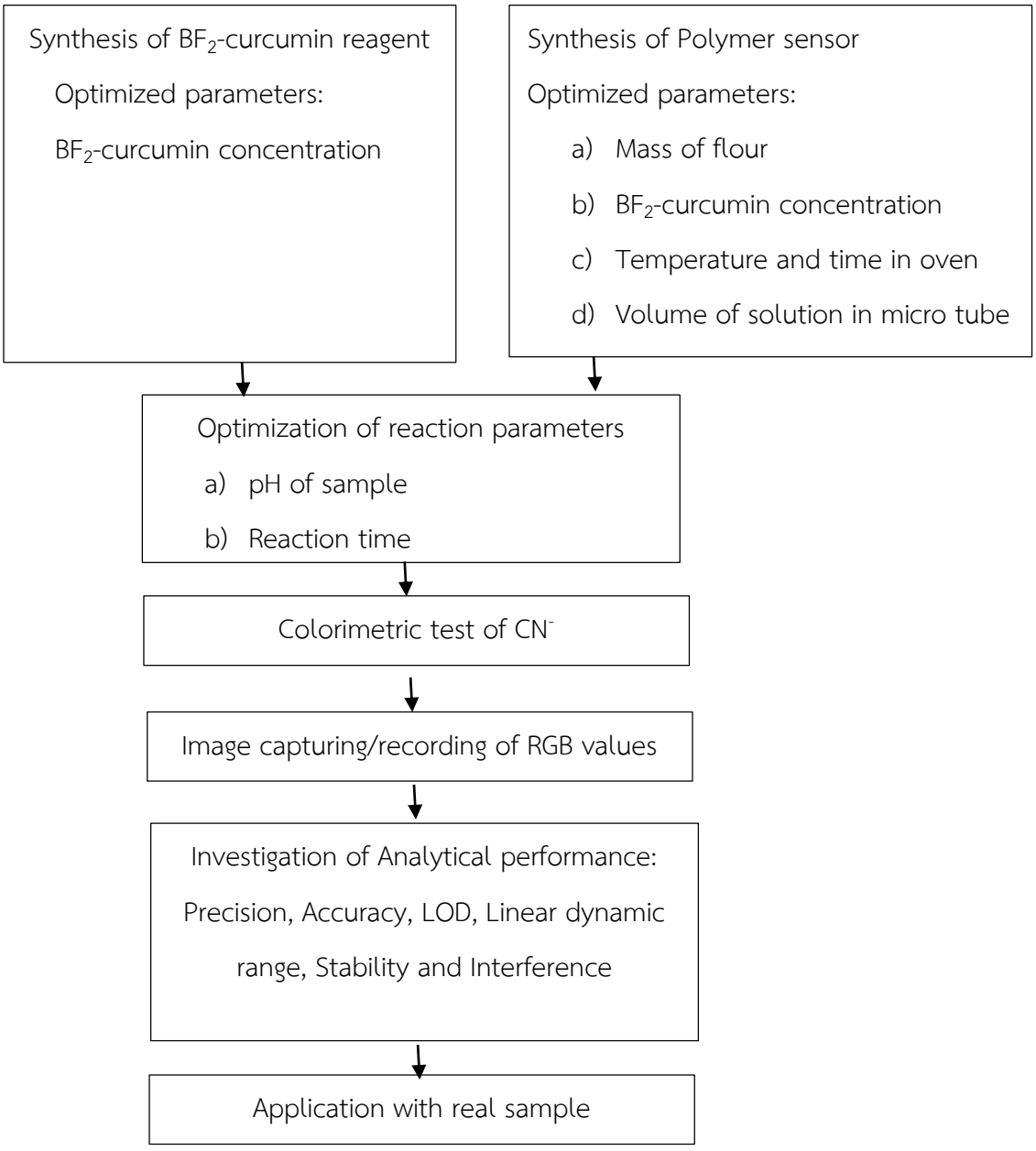

Fig 3.1 Experimental diagram

3.2 Part 1: Synthesis of BF_2-Curcumin reagent and BF_2-Curcumin synthesized starch film

3.2.1 Synthesis of BF_2-Curcumin reagent

a) 0.6 mL Borontrifluoride was added to 1 gram of dry turmeric powder which has been previously dissolved in 1 mL methanol.
b) The solution was refluxed at 60 °C for 2 hours in a sonicator and then cooled down to room temperature.
c) 0.5 g of the dry product was obtained and dissolved in 3 mL of acetone. The mixture was subsequently subjected to evaporation to obtain a dry crude product of BF_2-curcumin.
d) The crude product was dissolved in 60% ethanol to obtain 1 mM BF_2-curcumin concentration.
e) BF_2-curcumin concentration was in the range of 0.2 – 7 mM and then the final reagent was reacted with 10 mg/L CN^-. The effect on color intensity was investigated to obtain the optimum BF_2-curcumin concentration.

3.2.2 BF_2-curcumin synthesized starch film (Polymer sensor)

1.0 g of starch (tapioca flour) was dispersed in 10 mL of deionized water. The solution was heated on hot plate under continuous stirring until a clear sticky solution without sediments was obtained. The synthesis of the BF_2-curcumin embedded in the polymer procedure is as follows:

a) 1 mL of BF_2-curcumin reagent solution was mixed with 2.5 mL of starch solution.

b) 100 mL of the solution was pipetted into 1.5 mL micro tube.

c) The solution in the micro tube was kept in an oven for 90 minutes at 60 °C to obtain a solid film product.

3.2.3 Optimization of parameters affecting to BF_2-curcumin synthesized starch film

a) Mass of flour: The optimum BF_2-concentration obtained during the synthesis of the reagent was fixed to investigate the optimum mass of flour. Mass of flour was varied between the ranges of 0 - 0.8 g.
b) BF_2-curcumin concentration: The optimum mass of flour was fixed to investigate the right concentration of reagent needed to be anchored into the molecular structure of polymer for subsequent experiment. Concentration of BF_2-curcumin solution was varied in a range of 0.2 - 8 mM.
c) Temperature in the oven: The temperature at which the sensor was kept in an oven to obtain the dry product was varied in the range of 50 – 70 °C.
d) Time spent in oven: The time the sensor was made to stay in the oven was varied between 30 - 210 minutes to obtain the highest reaction product.
e) Volume of the mixture in PCR micro tube: Effect of the volume of the mixture (BF_2-curcumin and flour) in the micro tube on the color intensity was varied in the range of 25 – 150 mL.

3.3 Optimization of reaction parameters

The experimental results from the preliminary test showed that BF_2-curcumin concentration, pH of sample and reaction time were parameters which affected the reaction product. In view of this, they were investigated to obtain the maximum reaction product.

a) The effect of pH was investigated since pH of a sample normally varies from the source or type of water. The pH effect on the colorimetric product and also the RGB intensity was investigated by first testing the sensor against a blank solution at different pH (5, 6, 7, 8, 9, 10, and 11). This was to avoid any color interference during detection. Adjustment of the pH was made by the addition of 1 M NaOH and/or 1 M HCl.
b) Reaction time effect was studied in the range of 1-30 min after adding cyanide sample to the reagent.

3.4 Colorimetric test of CN^-

Hundred microliter of BF_2-curcumin reagent and/or BF_2-curcumin synthesized starch solution was placed in a 1.5 mL PCR micro-tube. The solutions were heated in an oven for 60 and 90 min respectively at 60 °C. One milliliters of 10 mg/L of CN^- solution was added to the test kits. The mixture was shaken and left until the color was visually observed. Each test was repeated by 3 samples and the RGB intensity of each sample was detected 6 times for an average calculation using Microsoft excel.

3.5 Image capturing system/ recording of RGB values

An iPhone 5s was used in obtaining digital image of the colored product throughout the experiment. A free of charge application (color assist) installed on the phone was used to measure and record the RGB intensity. The sample aperture on the phone was set to 5x5 pixels during measurement. A laboratory-built protective box (15 x 15 x 8.5 cm) was used during measurement to limit environmental light interference. The

black opaque box had a white interior with three LED light installed inside the box to serve as light source. The PCR micro-tube was made to hang on top of the protective box as a reaction container. A space with dimensions to that of the iPhone was made in the forefront of the protective box. A small narrow space was created within the provided space where the camera on the phone is fitted and fixed for image capturing and RGB measurement. The measured RGB values were transferred to an Excel spread sheet (2010 version) for subsequent data analysis.

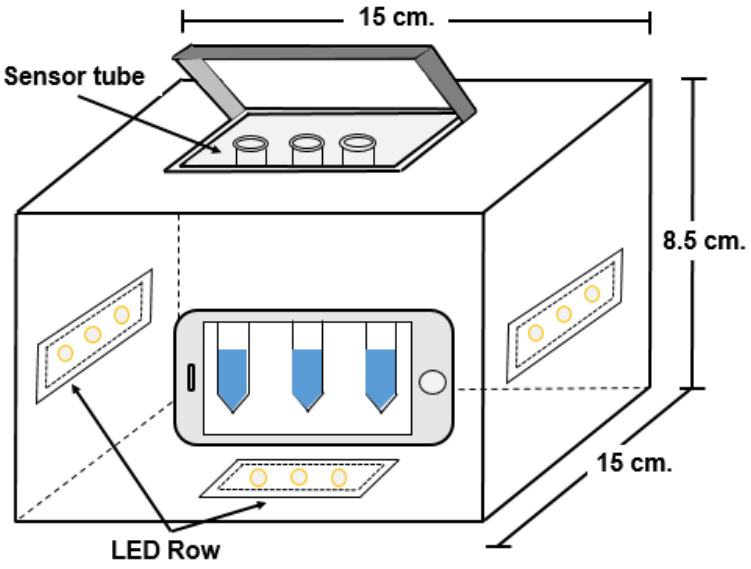

Figure 3.2 Color analytical system for cyanide detection.

3.6 Analytical performance

The optimized parameters were used to investigate the analytical performance of the proposed method by evaluating the linear calibration range. The analytical parameters considered are:

a) Linear dynamic range
b) Limit of detection
c) Precision (intra-day and inter-day)
d) Accuracy
e) Interference

3.6.1 Limit of detection: Stock solution of CN^- was prepared at 100 mg/L. A series of standard solutions in the range of 0.2 to 50 mg/L were prepared by diluting the stock solution (100 mg/L) with deionized water. Each CN^- standard solution was made to react with the test kits *i.e.* BF_2-curcumin reagent and BF_2-curcumin synthesized starch film. The RGB values of the blue product were measured and photographed by the use of a mobile phone and a laboratory protective box. The analytical data was used to generate the calibration equation of each color and also used to investigate the performance of the linear range. The results from the RGB calibration graphs were applied for calculating the limit of detection by standard method. The limit of detection was defined as the analyte concentration giving a signal equal to the blank signal, $y_{B,}$ plus three standard deviations of the blank, S_B: Limit of detection= $y_B + 3S_{B,}$ where y_B will be the intercept of calibration curve and S_B will be the standard deviation of blank (Miller and Miller, 2010).

3.6.2 Precision: The relative standard deviation percentage (%RSD) of each RGB value from the various replicates was used to estimate the precision of the method in both terms of intra-day and inter-day.

3.6.3 Accuracy: Accuracy was express as a percentage of relative error ((x_e-x_{known})/x_{known}*100) obtained by analyzing standard cyanide solution of an unknown with those quantified by an external calibration curve (x_e).

% Relative Error= [(measured concentration - true concentration)/ true concentration)] × 100.

3.6.4 Absorbance: The molecular absorption of each color product was also investigated by calculating the absorbance at each concentration using the eq. (1)

$$Ax = -\log \frac{(I_X - I_{X,b})}{(I_{x,w} - I_{x,b})} = -\log \frac{(I_x)c}{(I_{x,w})c} = -\log R_x \qquad (1)$$

Where for each color (R, G, B), A_X was absorbance of X, I_X was intensity of X, $I_{X,B}$ was the intensity of black ($I_{X,B}$ =0), $I_{X,W}$ was the intensity of white ($I_{X,W}$ = 255), and R_X was the reflectance of light X and C was the concentration of X (Kompany-Zareh, *et al*., 2002).

3.6.5 Stability: Several BF_2-curcumin reagent and/or polymer sensor were prepared at the same time to investigate their stability. The test kits were split into two groups with one part stored in a desiccator whereas the other part stored under room temperature. Three test kit from each group were removed for cyanide (20 mg/L) detection over a period of two months.

3.6.6 Investigation of interference anions: The influence of other extraneous anions (Cl^-, NO_3^-, SO_4^{2-}, and PO_4^{3-}) were investigated by keeping the concentration of CN^- in a solution fixed. Different concentrations of the individual interfering anions at different times were added to the fixed CN^- solution. The RGB intensity was measured after each addition to check the pattern of the curve. In addition, the colorimetric product upon the addition of anions were also investigated by comparing it to the zero concentration of the interfering anions.

3.7 Analysis of real sample by proposed method and standard spectrophotometric method.

The proposed method was applied to test real water samples from an abandoned tin mine site in Phuket-Thailand. The results obtained were compared to that of the standard spectrophotometer methods.

3.7.1 Spectrophotometric (colorimetric) method

1 Preparation of reagent

a) Sodium hydroxide dilution solution: 1.6 g of sodium hydroxide was dissolved in 1 L deionized water.

b) Chloramine – T solution: 1.0 g of white, water soluble chloramine – T solution was dissolved in 100 mL of DI water and was kept under refrigeration until it was ready to be used.

c) Acetate buffer: 8.2 g of sodium acetate trihydrate ($NaC_2H_3O_2.3H_2O$) was dissolved in 10 mL of DI water. The pH of the solution was adjusted to 4.5 by using glacial acetate acid.

2 Preparation of color reagent (Pyridine – barbituric acid reagent)

a) 15 g of barbituric acid was placed in a 250 mL volumetric flask. Just enough water was added to wash the sides of the flask and wet barbituric acid.

b) 15 mL of pyridine was added to the barbituric acid in the 250 mL volumetric flask.

c) 15 mL of concentrated HCl solution is subsequently added to the mixture in the flask. The mixture was therefore mixed and allowed to cool to room temperature.

d) The mixture is diluted to the 250 mL mark with deionized water.

3 Calibration and standardization

a) Series of standard cyanide solutions (0.2 – 1.3 mg/L) were prepared
b) 20 mL of each solution was pipetted into a 50 mL volumetric flask and diluted to 40 mL with sodium hydroxide dilution solution
c) 40 mL NaOH dilution solution was used as blank
d) Portion of each concentration and the sample were pipetted into different 50 mL volumetric flask and diluted to 40 mL with NaOH.
e) 1 ml of acetate buffer and 2 ml of chloramine-T solution were added to each solution and made to stand for 2 minutes after mixing.
f) 5ml of pyridine-barbituric acid reagent was added to each solution. Each solution was subsequently diluted to volume with distilled water.
g) The absorbance of each solution was measured after 8 minutes using NaOH as blank.
h) A graph of absorbance against cyanide concentration were made to quantify the amount of CN^- in the real sample.

3.7.2 Proposed method (BF_2-curcumin reagent and BF_2-curcumin synthesized starch film test kits)

a) Standard addition was performed on each sample by preparing cyanide solutions at different concentrations.
b) Each concentration from each sample was tested with the synthesized reagent and also BF_2-curcumin synthesized starch film test kits.
c) Each concentration and the measured intensity was used to prepare standard curve to quantify the unknown concentration.

CHAPTER 4

Results and Discussion

4.1 synthesis of BF_2-curcumin reagent

4.1.1 The effect of BF_2-curcumin concentration

The major problem of analytical techniques was an application of excessive and expensive chemicals. Thus, the method with minimized reagent was attractive for user. In this study, BF_2-curcumin concentration was varied within the range of 0.2 – 7 mM with volume of each concentration fixed at 100 microliters. Each concentrations was tested with 1 mL of 10 mg/L cyanide solution. The results are represented in Fig. 4.1

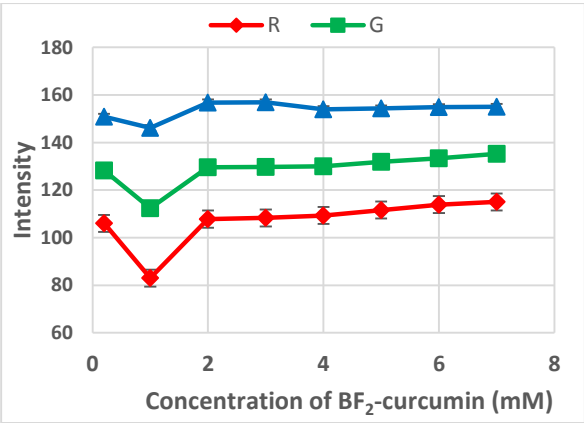

Fig 4.1 The effect of BF_2-curcumin concentration on RGB intensity in the presence of 10 mg/L cyanide solution.

As shown in Fig. 4.1, the blue intensity (I_B) provided the highest intensity followed by green (I_G) and red (I_R) respectively. This observation was ascribed to the fact that, the reaction product color was blue. The reflection of blue was therefore highest among the others. When the concentration of BF_2-curcumin was increased from 0.2 mM to 1 mM, the intensity of the three colors were decreased. This phenomenon was responsible for the higher product concentration related to the lower light reflection. The RGB intensity however increased after 2 mM BF_2-curcumin concentration. This indicated the unstabilized reaction product at excess concentration of BF_2-curcumin. For this reason, 1 mM BF_2-curcumin was chosen for all further experiment.

4.1.2 The effect of sample pH

The pH of a sample normally varies from the source and type of water. In view of this, the effect of cyanide sample pH was studied in the range of 7 – 12. Adjustment of the pH was made by the addition of 1 M NaOH and/or 1 M HCl. BF_2-curcumin reagent was first tested against 1 mL of blank solution at different pH. This was to assure the stability of the reagent to pH change. The results were shown in Fig 4.2.

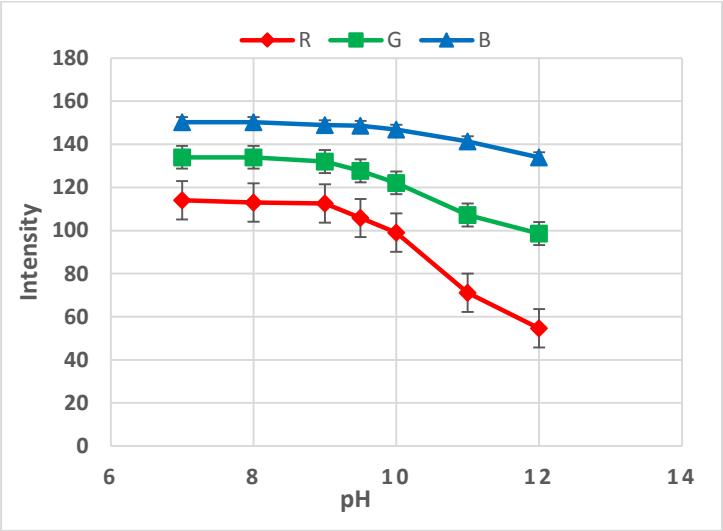

Fig 4.2 Effect of pH on RGB intensity in the presence of 1 mL blank sample.

As represented in Fig. 4.2, the measured intensity (I_R, I_G, I_B) from the blank test remained unchanged within the ranges of 7 - 9. However, the RGB intensity began to decrease after pH 9 corresponding to the formation of a blue color product. Fall in the intensity after pH 9 was ascribed to an increased in light absorption of the blank blue product which in turn resulted a decrease in reflectance. This observation indicated the unstability of BF_2-curcumin extract at pH > 9. The pH 7, 8 and 9 which did not show any color upon the reaction with the blank sample were subsequently tested with different cyanide concentration. As illustrated in Fig. 4.3, the digital image showed the less intense of color at pH 7 and 8, even when high concentration of 5 mg/L cyanide was applied. Sample pH was therefore fixed at 9 and used in further experiment to avoid any effect of pH change.

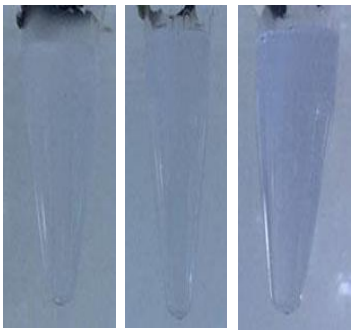

pH 7 pH 8 pH 9

Fig 4.3 Digital image of colored product of 5 mg/L cyanide sample and BF_2-curcumin at pH 7, 8 and 9.

4.1.3 The effect of reaction time

Since quantitative analysis from colorimetry is highly dependent on the intense of color product, the reaction rate and time was important to efficiency and precision of detection by the method. In this research, the effect of reaction time was varied from 1 – 30 minute.

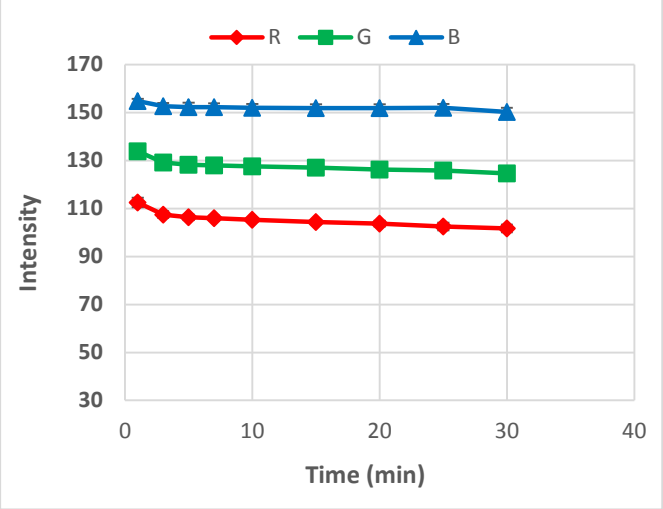

Fig 4.4 Relationship between RGB intensity and reaction time in the presence of 10 mg/L cyanide solution.

After the addition of CN^- solution into the 1.5 mL reaction tube, the mixture was shaken and left to settle. The solution immediately displayed a faint blue color which could be observed with the naked eye and became darker with time. This was agreed with the results in Fig. 4.4. The RGB intensity decreased with increasing reaction time from 1 – 5 min. However, there was significantly no effect of reaction time on the color intensity over 5 min. These referred to the high reaction rate between CN^- and BF_2-curcumim. Based on this observation and results from Fig. 4.4, readings of RGB intensity values for quantitative analysis were made in the time frame of 5 min after adding CN^- to the BF_2-curcumin reagent.

The optimum conditions which gave the highest reaction product (*i.e.* least intensity) were found to be 1 mM BF_2-curcumin concentration, pH 9 of sample and 5 minutes reaction time.

4.2 Colorimetric reaction of cyanide with the reagent

The reaction of cyanide solution and BF_2-curcumin resulted in the formation of blue color product which became darker with increasing cyanide concentration. This could be observed with the naked eye. The formation of the colored product was attributed to the deprotonation of the hydroxyl group of BF_2-curcumin. The BF_2-curcumin consist of two methoxy phenol groups as electron donor parts conjugated to the difluoroboron enolate as the electron acceptor Fig. 4.5. Cyanide ion has the tendency to deprotonate the hydroxyl moiety of BF_2-curcumin molecule. This is because, CN^- in water is normally present as oxyanions with relatively low acid dissociation constant. The negative charges produced could then delocalize to the acceptor part resulting in the change of BF_2-curcumin color.

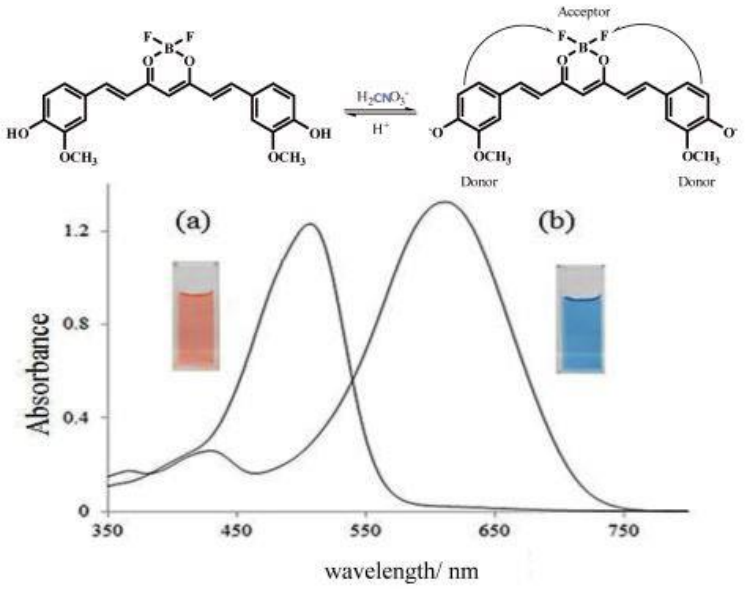

Fig 4.5 The color change mechanism of BF_2-curcumin upon addition of CN^- and the UV-visible spectra of (a) BF_2-curcumin solution and (b) in the presence of 20 mg/L of CN^-.

As shown in Fig. 4.6, there was significantly no change in the blue color product at concentration of CN^- above 30 mg/L. It was assumed that the complete deprotonation of the BF_2-curcumin molecules in the solution was established and that no change was obtained thereafter. However, there was some significant change in the measured RGB intensity values after 50 mg/L CN^- concentration as show in Fig. 4.7(a) even though the colorimetric product remained unchanged. It was assumed that excess CN^- concentration after complete deprotonation of the reagent was latent in the solution and however increased the absorptivity of the solution. This observation corresponded to the decrease in RGB intensity values as the concentration was increased after 50 mg/L.

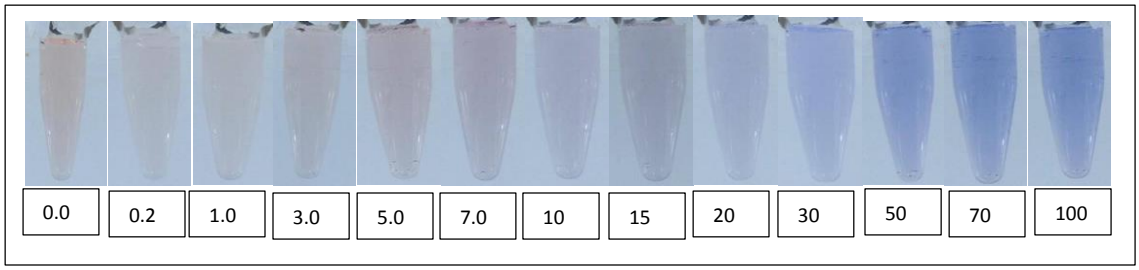

Fig 6 Colorimetric products obtained from reaction with various concentration of cyanide solution (0.2 to 50 mg/L).

4.3 Digital image analysis for quantification of cyanide

Obtaining analytical data in the form of RGB values from the colorimetric product was basically by virtue of the digital image received from a standard trichromatic response of a particular image. The RGB intensity data produced a value ranging from 0 to 255 for each channel. That is, in the absence of any environmental interferences a black digital image will produce an R, G, B value of 0, 0, 0 respectively whereas a white digital image will produce R, G, B value of 255, 255, 255 respectively. This

phenomenon conforms to the idea that a black digital image absorbs all the light intensity directed towards it whereas a white digital image reflects all light intensity directed towards it. In addition, the colors obtained from each of the three channels were subtractive colors and selectively absorb certain wavelength of light, thus affecting the observed eye.

The optimum parameters, *i.e.* sample pH of 9, 1 mM BF_2-curcumin concentration and 5 min reaction time were used to investigate the relationship between the RGB intensity and different CN^- concentration (0.2 - 100 mg/L). The blue color product generated by the reaction could be related to the concentration of CN^- present facilitating the development of an objective semi analytical methodology. As presented in figure 4.7(a), the RGB intensity values obtained were inversely related to the concentration of CN^-. This was attributed to the reaction product formation leading to a decrease in light reflectance. The blue intensity was the highest followed by green and red respectively. The difference between the individual intensity became obvious and distinct as the concentration of CN^- was increased and presented as a dark colored product. The highest sensitivity was observed by the red component (slope of 2.2788 a.u. L/mg) as shown in Fig. 4.7(b) as the slope of the linear dynamic range equation. This observation was basically because, the RGB colors are subtractive color from primarily absorbed object. Consequently, the blue product from cyanide reaction could highly absorbed the green component. Green is a complementary color of blue and thus a high absorbance of this color was expected given the presumptive test color was blue. This findings corresponded to results obtained from spectrophotometry, which showed the highest absorbance in red wavelength region of 578 nm. The linear response was distinctly observed in the concentration range of 0.2 - 7 mg/L.

The absorbance at each concentration of the colored product was also investigated by calculating the absorbance from the intensity using the equation described by Kompany-Zareh *et al*. (2002). On the contrary to the RGB intensity, the obtained RGB absorbance values showed a direct relationship with CN^- concentration as shown in Fig. 4.7(c). This observation was related to the high absorption of light by highly concentrated

reaction product which corresponded to the dark color product. The absorbance of red color was higher than green and blue Fig. 4.7(c). This observation also conforms to the inverse relationship between intensity and absorbance.

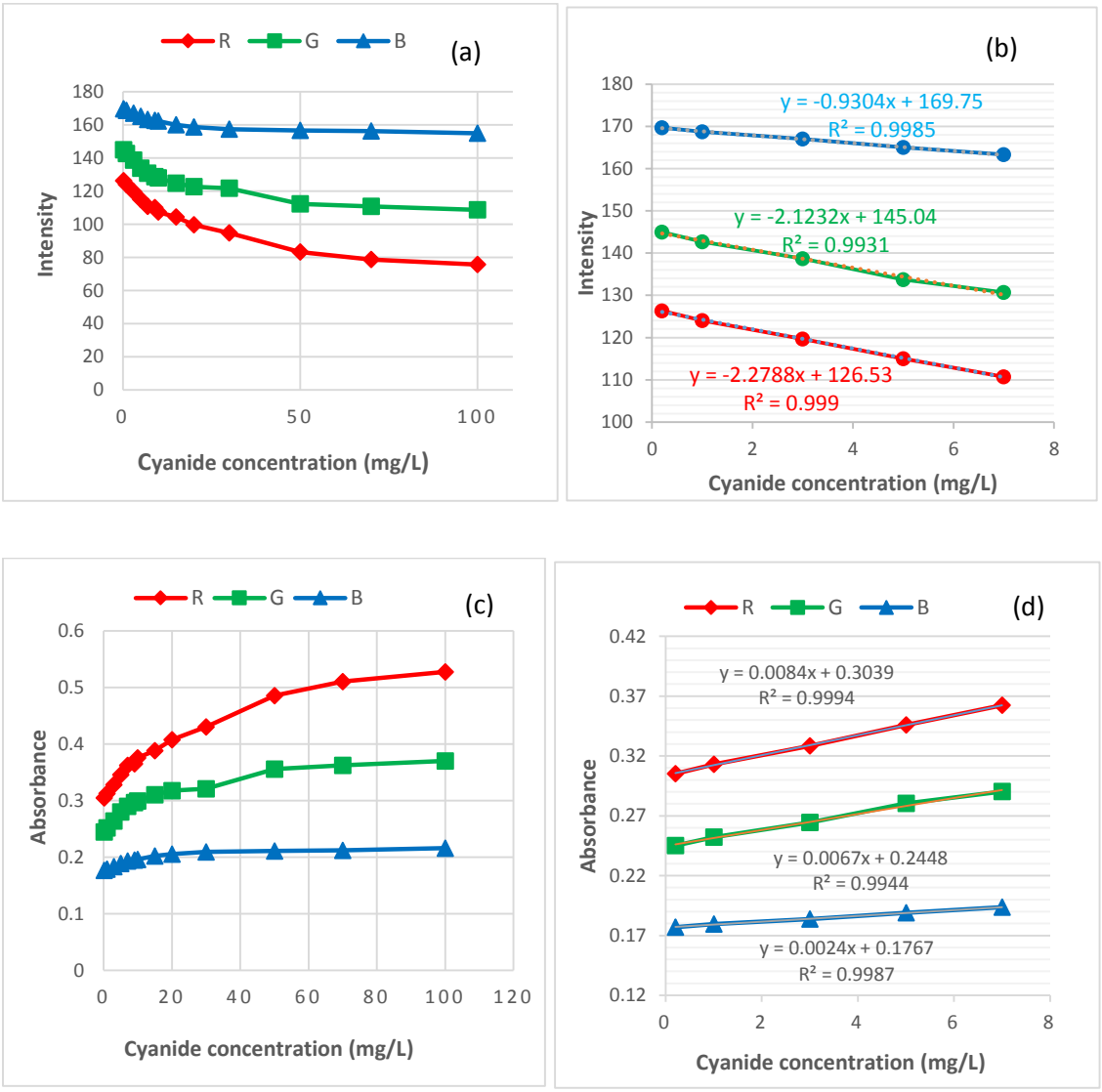

Fig. 4.7 Relationship between cyanide concentration and (a) individual RGB intensity values (b) linear range (0.2 - 7 mg/L) (c) calculated absorbance (d) linear range (0.2-7 mg/L).

As presented in Fig. 4.7(d) as the slope of each equation, the highest sensitivity of the calculated absorbance was again observed by the red component (highest slope of 0.0084 a, u. L/mg) in the positive direction, contrary to that of the RGB intensity which was observed in the negative direction. Likewise to the RGB intensity, the linear response of absorbance was distinctly observed in the range of 0.2 - 7 mg/L.

4.4 Total intensities and absorbance of colored product

Relationship between the total intensity, total absorbance and CN^- concentration were also investigated. This was because, in digital colorimetry the color of the reaction product is obtained by the combination of RGB data. The total intensity which is represented by I_{TOTAL}, was defined as $I_R + I_G + I_B$ and total absorbance which was represented by A_{TOTAL}, was defined as $A_R + A_G + A_B$. The relationship between I_{TOTAL} and A_{TOTAL} with CN^- concentration are presented in Fig. 4.8

With regards to the linear dynamic range, both the individual and total values (I_{TOTAL} and A_{TOTAL}) covered the same liner range *i.e.* 0.2 – 7 mg/L sample concentration. However the sensitivity of the total RGB intensity and absorbance turned to be higher than those of the individual values. The sensitivity of the RGB intensity were higher than that of the absorbance. This means that, I_{TOTAL} has higher ability to distinguish between similar CN^- concentrations compared to A_{TOTAL}.

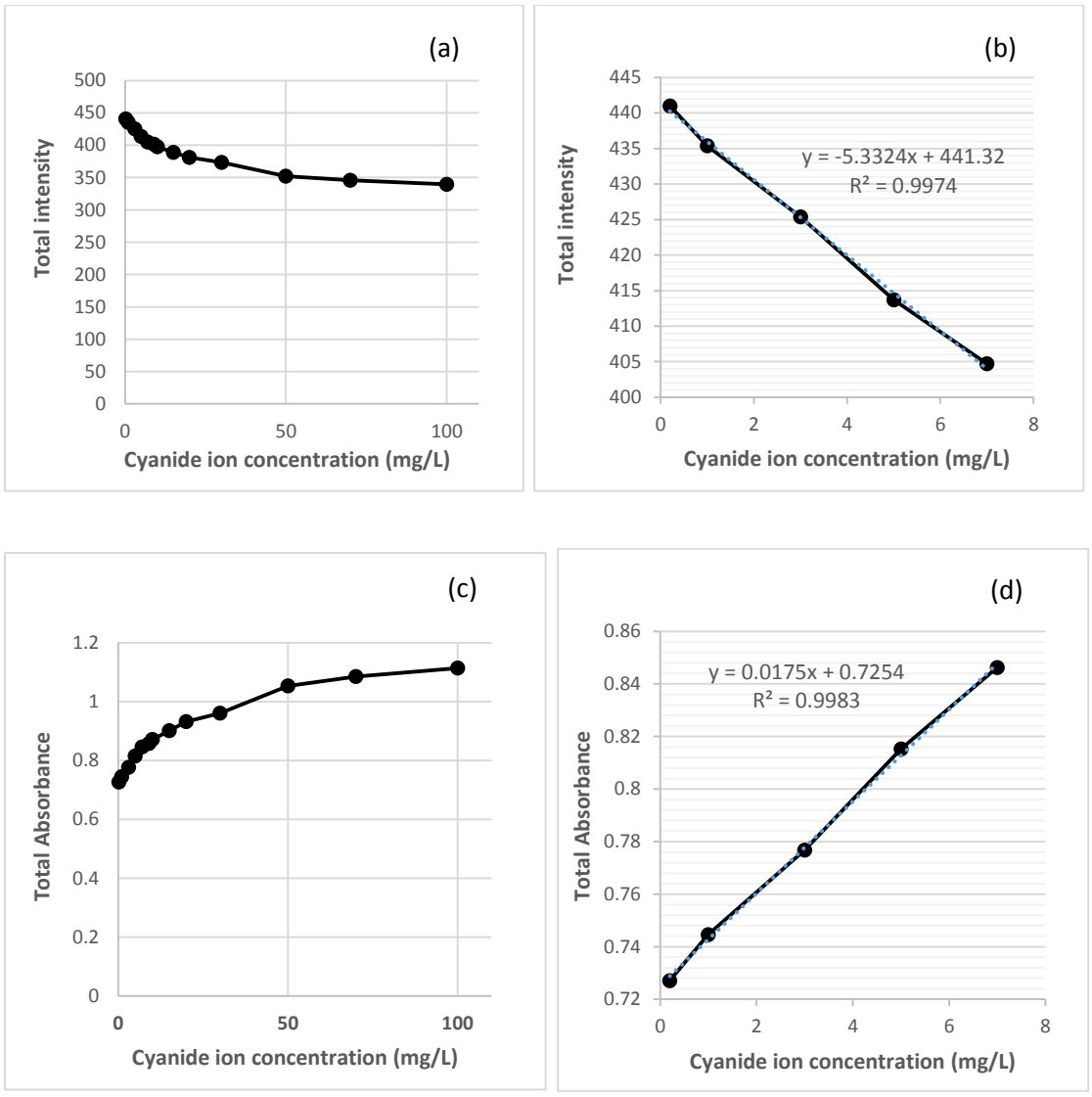

Fig 4.8 Relationship between cyanide concentration and (a) I_{TOTAL} (b) linear range of I_{TOTAL}, (c) A_{TOTAL} (d) linear range of A_{TOTAL}.

4.5 Blank subtracted RGB values

Sample matrix or source of sample can affect to the RGB values of the colorimetric product. In order to avoid the interference of the sample matrix, the RGB value of the blank was taken into account during the investigation of the analytical performance of this proposed method. The RGB value of the blank was subtracted from the individual values. The relationship between the subtracted RGB values and CN^- concentration both as intensities and their absorbance were presented in Fig 4.9

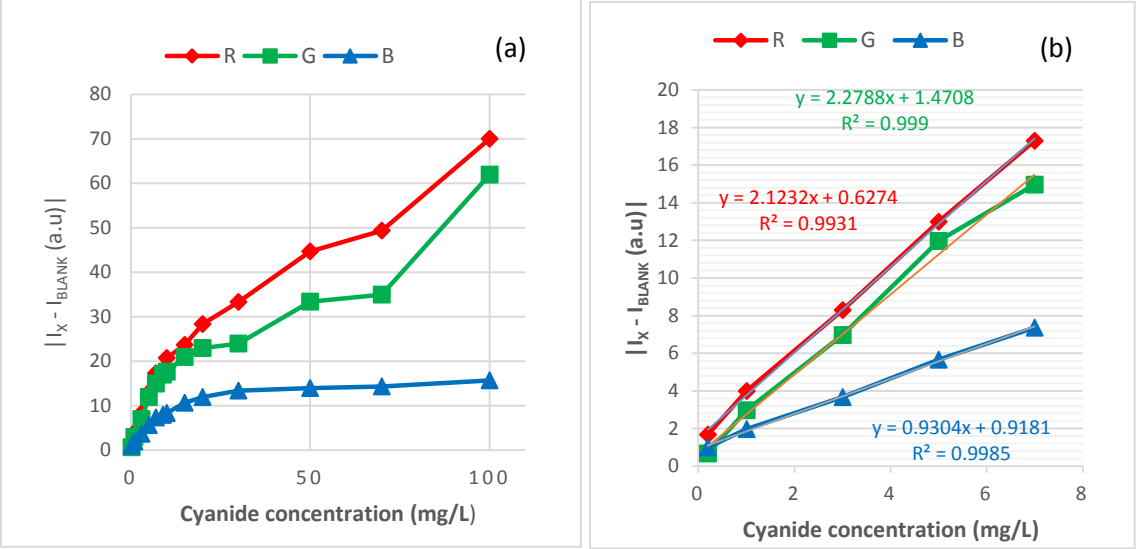

Fig 4.9 Relationship between blank subtracted RGB values and cyanide concentration (a) individual intensity (b) linear range for blank subtracted individual intensity (c) individual absorbance (d) linear range for blank subtracted individual absorbance.

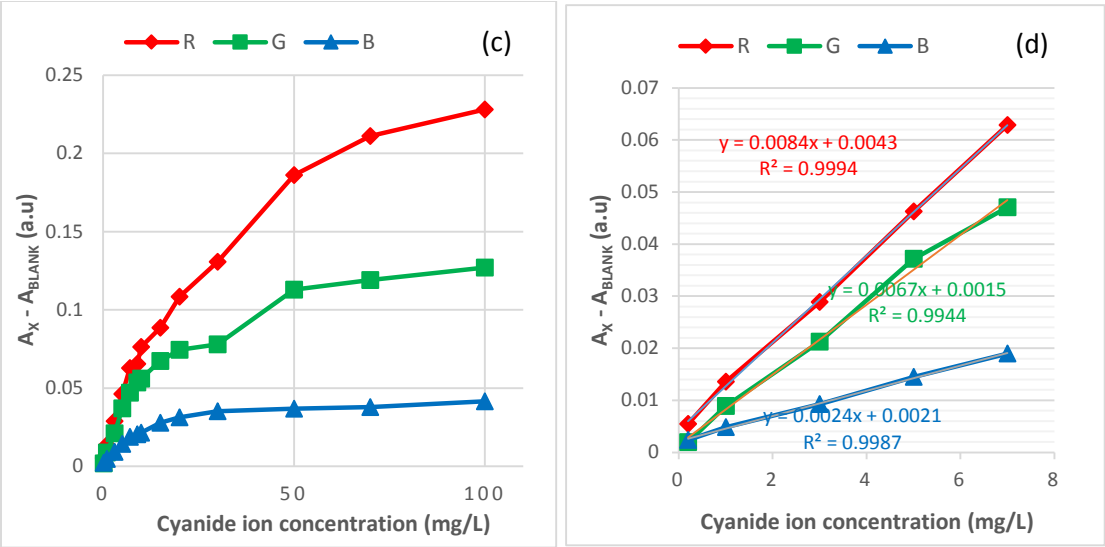

Fig 4.9 Relationship between blank subtracted RGB values and cyanide concentration (a) individual intensity (b) linear range for blank subtracted individual intensity (c) individual absorbance (d) linear range for blank subtracted individual absorbance. (Conti.)

As presented in Fig 4.9 (a) and (b), the intensity of the blank subtracted RGB values decreased with increased cyanide concentration whereas the absorbance of the subtracted RGB values increased with increased cyanide concentration. Furthermore, the blank subtraction of the RGB values showed the same sensitivity as that of the original individual intensity. The total blank subtraction from the total RGB intensity and absorbance were also considered to investigate the analytical performance of this method. The results were presented in Fig 4.10.

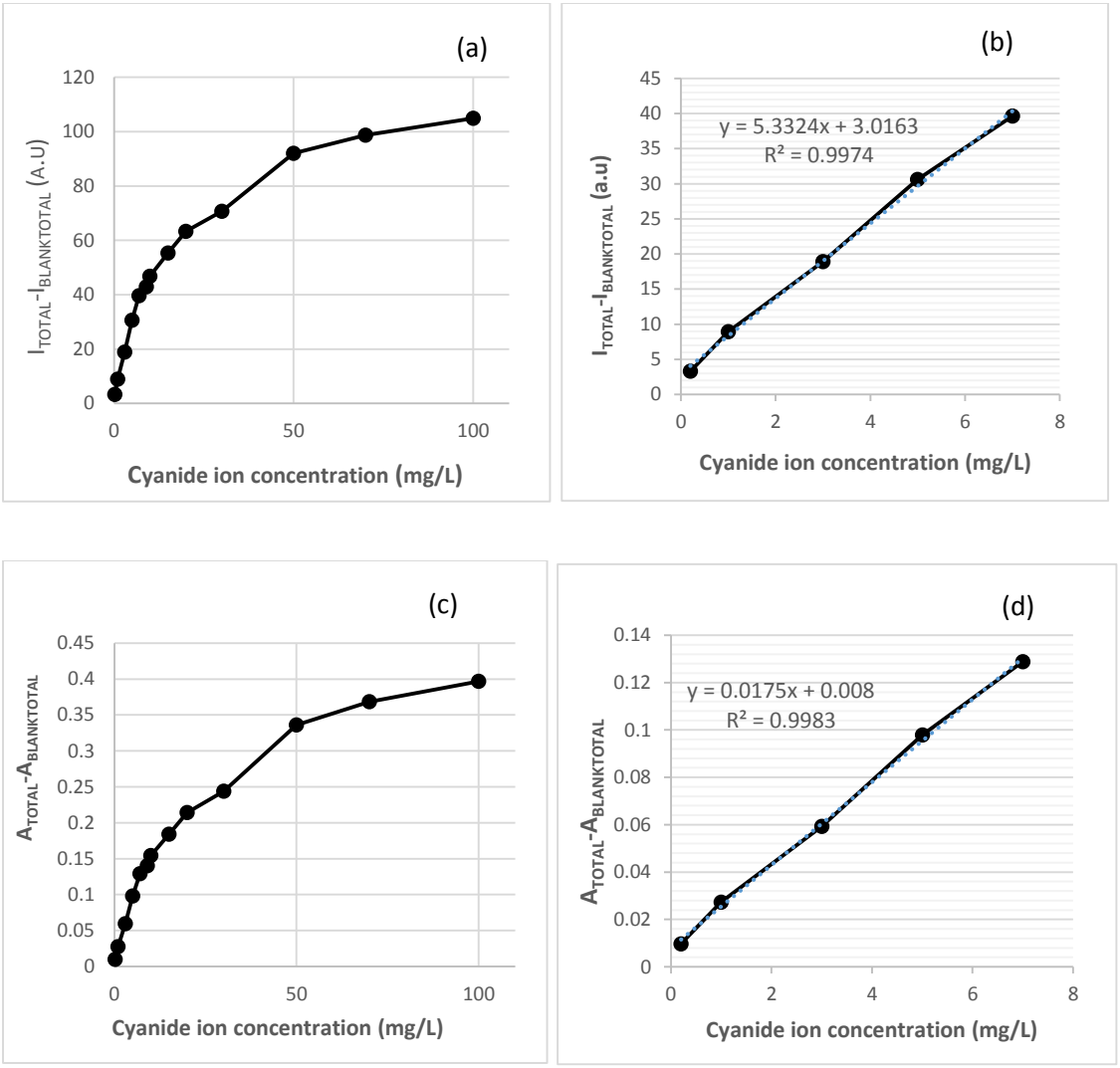

Fig 4.10 Relationship between blank subtracted RGB values and cyanide concentration (a) total intensity (b) linear range of total intensity (c) total absorbance (d) linear range of total absorbance.

As shown in Fig. 4.10, the total intensity and absorbance gave the same sensitivity to that of the subtracted total blank from the total intensity and absorbance i.e. I_{TOTAL} - I_{BLANK} and A_{TOTAL} - A_{BLANK}. This observation shows clearly that, there was significantly no interference of the sample matrix with regards to this method**.** In addition,

the green color component demonstrated the highest sensitivity repeating the result when the individual RGB values were considered (Table 4.1).

4.6 Analytical performance and method validation

The analytical performances including calibration equation, linear dynamic range and linearity of the proposed is summarized in table 1. Whiles other parameters are shown in table 2.

Table 4.1. Calibration equation, sensitivity, linear range and correlation coefficient for the detection of cyanide by BF_2-curcumin reagent.

Relationships	Linear range (mg/L)	Calibration equation	R^2
I_R and C	0.2-7	y = (-2.279 ± 0.04)x+ (126.55 ± 0.2)	0.9990
I_G and C	0.2-7	y = (-2.123 ± 0.1)x+ (145.04 ± 0.4)	0.9931
I_B and C	0.2-7	y = (-0.930 ± 0.02)x+ (169.75 ± 0.09)	0.9985
A_R and C	0.2-7	y = (0.008 ± 0.0002)x+ (0.3039 ± 0.0005)	0.9994
A_G and C	0.2-7	y = (0.007 ± 0.0003)x+ (0.2448 ± 0.001)	0.9944
A_B and C	0.2-7	y = (0.002 ± 0.00006)x +(0.1767 ± 0.0002)	0.9987
I_{TOTAL} and C	0.2-7	y = (-5.332 ± 0.2)x+ (441.32 ± 0.6)	0.9974
A_{TOTAL} and C	0.2-7	y = (0.018 ± 0.0004)x+ (0.7254 ± 0.0017)	0.9983
I_R - I_{Rblank} and C	0.2-7	y = (-2.279 ± 0.04)x- (1.4708 ± 0.2)	0.9990
I_G - I_{Gblank} and C	0.2-7	y = (-2.123 ± 0.1)x- (0.6274 ± 0.4)	0.9931
I_B - I_{Bblank} and C	0.2-7	y = (-0.930 ± 0.2)x- (0.9181 ± 0.09)	0.9985
A_R - A_{Rblank} and C	0.2-7	y = (0.008 ± 0.0001)x+ (0.0043 ± 0.0005)	0.9994
A_G - A_{Gblank} and C	0.2-7	y = (0.007 ± 0.0003)x+ (0.0015 ± 0.001)	0.9944
A_B - A_{Bblank} and C	0.2-7	y = (0.002 ± 0.0006)x+ (0.0021 ± 0.0002)	0.9987
(I_R -I_{Rblank}) + (I_G - I_{Gblank}) + (I_B - I_{Bblank}) and C	0.2-7	y = (-5.332 ± 0.2)x- (3.0163 ± 0.6)	0.9974
(A_R -A_{Rblank}) + (A_G - A_{Gblank}) + (A_B -A_{Bblank}) and C	0.2-7	y = (0.018 ± 0.0004)x+ (0.008 ± 0.002)	0.9983

Table 4.2. Limit of detection, accuracy and precision of BF_2-curcumin reagent.

Relationships	LOD (mg/L)	Accuracy			Precision (%RSD)	
		Known (mg/L)	Measured (mg/L)	%Relative error	Intra-day	Inter-day
I_R and C	0.31 ± 0.006	4	4.05	1.26	0.90-2.30	0.74-1.10
I_G and C	0.81 ± 0.039	4	4.12	2.91	0.30-1.06	1.00-1.17
I_B and C	0.38 ± 0.008	4	4.03	0.76	0.25-0.44	0.31-0.48
A_R and C	0.25 ± 0.004	4	3.97	-0.77	1.39-3.46	1.11-1.48
A_G and C	0.73 ± 0.032	4	4.07	1.66	0.71-2.40	1.88-2.28
A_B and C	0.40 ± 0.009	4	4.06	1.38	1.09-1.83	1.09-1.70
I_{TOTAL} and C	0.50 ± 0.015	4	4.07	1.83	0.36-1.00	0.50-0.78
A_{TOTAL} and C	0.40 ± 0.009	4	4.02	0.46	0.95-2.56	1.15-1.63
I_R - I_{Rblank} and C	0.31 ± 0.006	4	4.05	1.25	3.45-7.71	2.93-3.33
I_G - I_{Gblank} and C	0.81 ± 0.039	4	4.12	2.90	2.65-6.73	4.24-6.00
I_B - I_{Bblank} and C	0.36 ± 0.008	4	4.03	0.72	8.18-9.64	6.52-13.47
A_R - A_{Rblank} and C	0.25 ± 0.004	4	3.97	-0.66	3.77-8.65	3.10-3.66
A_G - A_{Gblank} and C	0.73 ± 0.032	4	4.08	1.90	2.65-7.15	4.64-6.38
A_B - A_{Bblank} and C	0.40 ± 0.009	4	4.06	1.43	8.22-9.79	6.37-13.51
(I_R -I_{Rblank}) + (I_G - I_{Gblank}) + (I_B - I_{Bblank}) and C	0.50 ± 0.026	4	4.07	1.82	2.97-6.65	3.86-4.06
(A_R -A_{Rblank}) + (A_G - A_{Gblank}) + (A_B -A_{Bblank}) and C	0.40 ± 0.021	4	4.02	0.46	3.18-7.39	3.57-4.34

The red channel provided the lowest limit of detection followed by blue and green respectively. This observation was common to both the intensity and the calculated absorbance. The blank subtracted RGB intensity and absorbance gave almost the same LOD as the original unsubtracted values (Table 2). Furthermore, the total RGB intensity and absorbance and the blank subtracted total RGB values gave the same LOD *i.e*. 0.50 ± 0.015 for I_{TOTAL} and $(I_R - I_{Rblank}) + (I_G - I_{Gblank}) + (I_B - I_{Bblank})$ and also 0.40 ± 0.021 for A_{TOTAL} and $(A_R - A_{Rblank}) + (A_G - A_{Gblank}) + (A_B - A_{Bblank})$. Accuracy in terms of % relative error $((x_e - x_{known})/x_{known}*100)$ estimated by analyzing a known standard solution (x_{known} = 4 mg/L) and quantification using external calibration (x_e) were overall excellent. The percentage relative error varied from 0.46 to 2.91% throughout the investigation. This indicated that, good accuracies were obtained for almost all measurement. Precision measured by %RSD of repetitive analysis (n = 6) was in the range of 0.25 – 3.46 %RSD for intra-day analysis and 0.31 – 2.28 %RSD for inter-day (over 5 days) with regards to the individual intensities and absorbance. Total intensity showed good precisions *i.e.* 0.36 – 1.00 and 0.50 – 0.78 %RSD for intra-day and inter-day intensity precision respectively. Total absorbance also gave good precision *i.e*. 0.95 – 2.56 and 1.15 – 1.63 %RSD for intra-day and inter-day absorbance precision respectively. However, the blank subtracted RGV values showed poor precision (Table 4.2). In view of this, precision was recommended to be made without the blank consideration.

4.7 Stability of BF_2-curcumin reagent

Several BF_2-curcumin test kits were prepared at the same time to investigate its stability. The test kits were split into two groups with one part stored in a desiccator and the other part stored under room temperature to study the effect of humidity. Three test kits were removed from each part for cyanide detection within a period of 1, 3, 7, 14, 21, 42 and 63 days. The RGB intensities from the test kits stored under

room temperature altered by 11.21%, 5.97% and 7.92% respectively throughout the experimental period (1 - 63 days) with reference to the least intensity recorded on the first day. The intensities measured on the first day gave the highest reaction product Fig. 4.11(a). The test kits stored under room temperature also altered by 10.57%, 5.72% and 5.70% respectively Fig. 4.11(b).

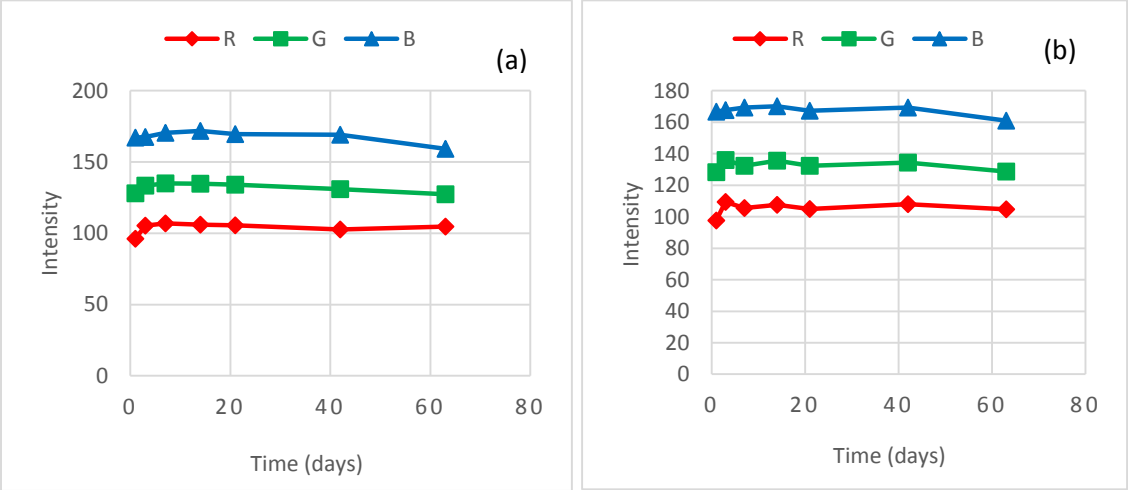

Fig 4.11 Stability of reagent stored under (a) room temperature (b) desiccator.

The results show insignificant difference between 2 storage conditions. It should conclude to recommend for ambient storage because of more convenient application. Also, the advantage of reagent sensor should be mentioned that are resistant to humidity effect and longtime shelf lite at least 3 months. It was recommended that the reagent was stored in a desiccator on the basis of the obtained results.

4.8 Interference

The sensing ability of the reagent was examined with Cl^-, NO_3^-, SO_4^{2-}, and PO_4^{3-}. These ions were selected because, they possess similar basicity to cyanide ion and easily form hydrogen bonding. This phenomenon tends to alter cyanide selectivity in several applications. The concentration of chloride and phosphate ions were varied in the range of 0 – 50 mg/L whereas that of nitrate and sulfate were in the range of 0 – 30 mg/L and 0 – 100 mg/L respectively. The results were represented in Fig. 4.12

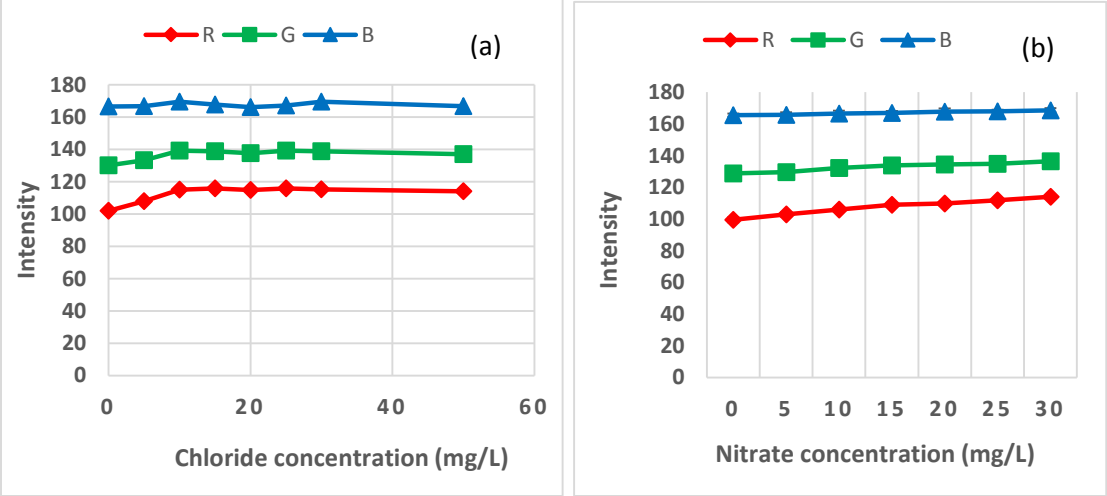

Fig. 4.12 Effect of interfering ions (a) chloride (b) nitrate (c) sulfate (d) phosphate, on the intensity of 20 mg/L CN^- solution.

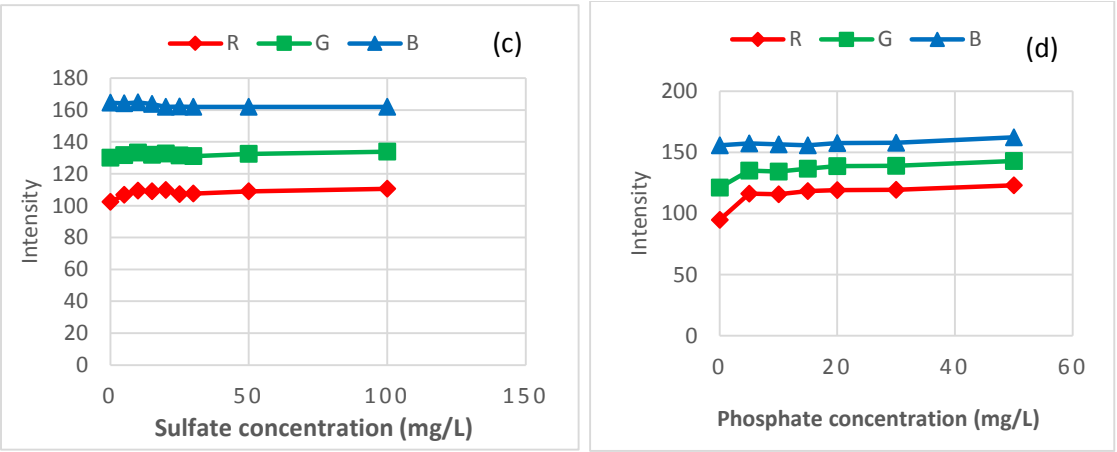

Fig. 4.12 Effect of interfering ions (a) chloride (b) nitrate (c) sulfate (d) phosphate, on the intensity of 20 mg/L CN^- solution. (conti.)

RGB intensity values were altered by 13.55%, 7.05%, and 1.94% respectively when different concentrations of chloride ions were added to 20 mg/L cyanide solution Fig. 4.12(a). The sensibility of cyanide against sulfate was also investigated and the RGB intensities measured changed by 8.10%, 2.91% and 1.78% respectively with reference to 0.00 mg/L sulfate concentration Fig. 4.12(b). The effect of nitrate on the sensibility of cyanide as shown in Fig 4.12(c) was altered by 14.68%, 5.95% and 1.88%. Finally the effect of phosphate on the intensity varied by 29.61%, 18% and 4.24%. Fig 4.12(d).

4.9 Quantification of CN^- in real sample

4.9.1 Quantification of CN^- concentration in real sample by standard spectrophotometer (colorimetric) method and BF_2-curcumin reagent

Water sample was obtained from an abandoned tin mine (de condo) site in Phuket-Thailand. Standard addition method was applied to the sample to assure the presence on cyanide. A calibration curve was made by preparing standard cyanide concentrations (0.2, 0.4, 0.6, 0.8 and 1 mg/L). The absorbance of each concentration was measured with a spectrophotometer and the results presented in Fig. 4.13

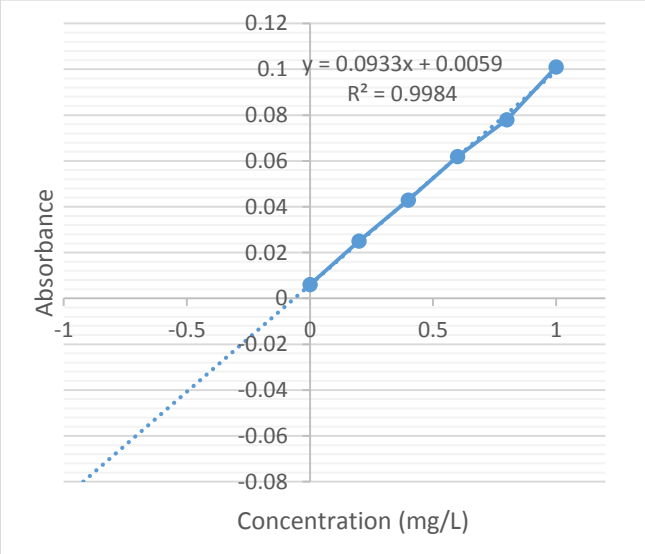

Fig 4.13 Relationship between absorbance and cyanide concentration in real sample from tin mine site using spectrophotometer.

By reversing the calibration equation and substituting the value of y by zero, it was found that 0.006 mg/L of cyanide was present.

The sample from the abandoned mine site was subsequently measured by the synthesized BF_2-curcumin reagent. The regent (BF_2-curcumin) in DI water

was used as blank. The RGB intensity value of the blank was measured and subsequently substituted in each calibration equation as y. The measured RGB intensity was plotted against different cyanide concentration (0.2, 0.4, 0.6, 0.8, and 1.0 mg/L) as presented in Fig. 4.14.

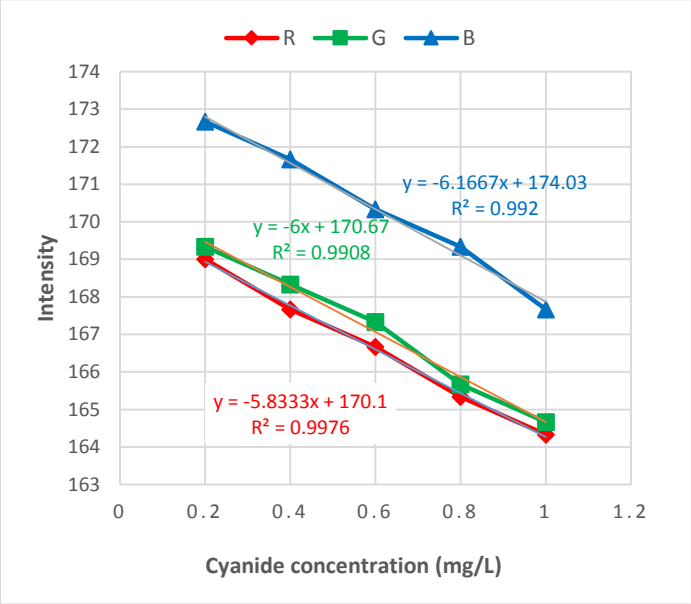

Fig 4.14 Relationship between RGB intensity and cyanide concentration in real from the abandoned tin mine site using BF_2-curcumin reagent.

The results obtained by each color channel from the linear range are presented in table 4.3. It was observed that, the green and blue color gave similar concentration of cyanide in the real sample.

Table 4.3 Quantification of cyanide in the real sample by BF_2-curcumin synthesized reagent.

Intensity	y= mx + c	y	m	c	calculated
R	y= -5.833x + 170.1	175.667	-5.833	170.01	0.9543
G	y= -6.x + 170.67	174.333	-6.000	170.67	0.6106
B	y= -6.1667x + 174.03	178.000	-6.167	174.03	0.6437

4.10 BF_2-curcumin synthesized starch film

Due to the advantages associated with the use of polymeric materials with chromogenic units embedded in their molecular structure such as specific selectivity of analyte and also their excellent film forming properties. It was of interest to incorporate BF_2-curcumin regent into the molecular structure of starch. Parameters affecting to the synthesis of BF_2-curcumin synthesized starch film and the reaction parameters between the sensor and cyanide sample were investigated. The parameters includes mass of starch, heating temperature and time spent in oven, reaction time and pH of sample.

4.10.1 Effect of Mass of flour

The optimum concentration of BF_2-curcumin obtained during the synthesis of the reagent in 4.1.2 was fixed to investigate the mass of flour which will give the highest reaction product. Mass of flour was initially varied between 0.2 – 2 g. It was observed that flour solutions of masses above 0.8 g were thick to the extent that they could not be pipetted by the micro pipette. For this reason, the mass of flour was narrowed to 0 - 0.8 g. 2.5 mL of each flour solution was mixed with 1 mL of 1 M BF_2-curcumin. Hundred microliters of the mixture was pipetted into a 1.5 ml micro tube which was then placed in an oven at 60 ^{o}C for 60 min. The synthesized test kit was made to react with 1mL 20 mg/L CN^- solution. It was observed that, the mixture with mass of flour

above 0.4 g were difficult to pipette due to their high viscosity. The effect of mass of flour on the colorimetric product and RGB intensity were presented in Fig 4.14.

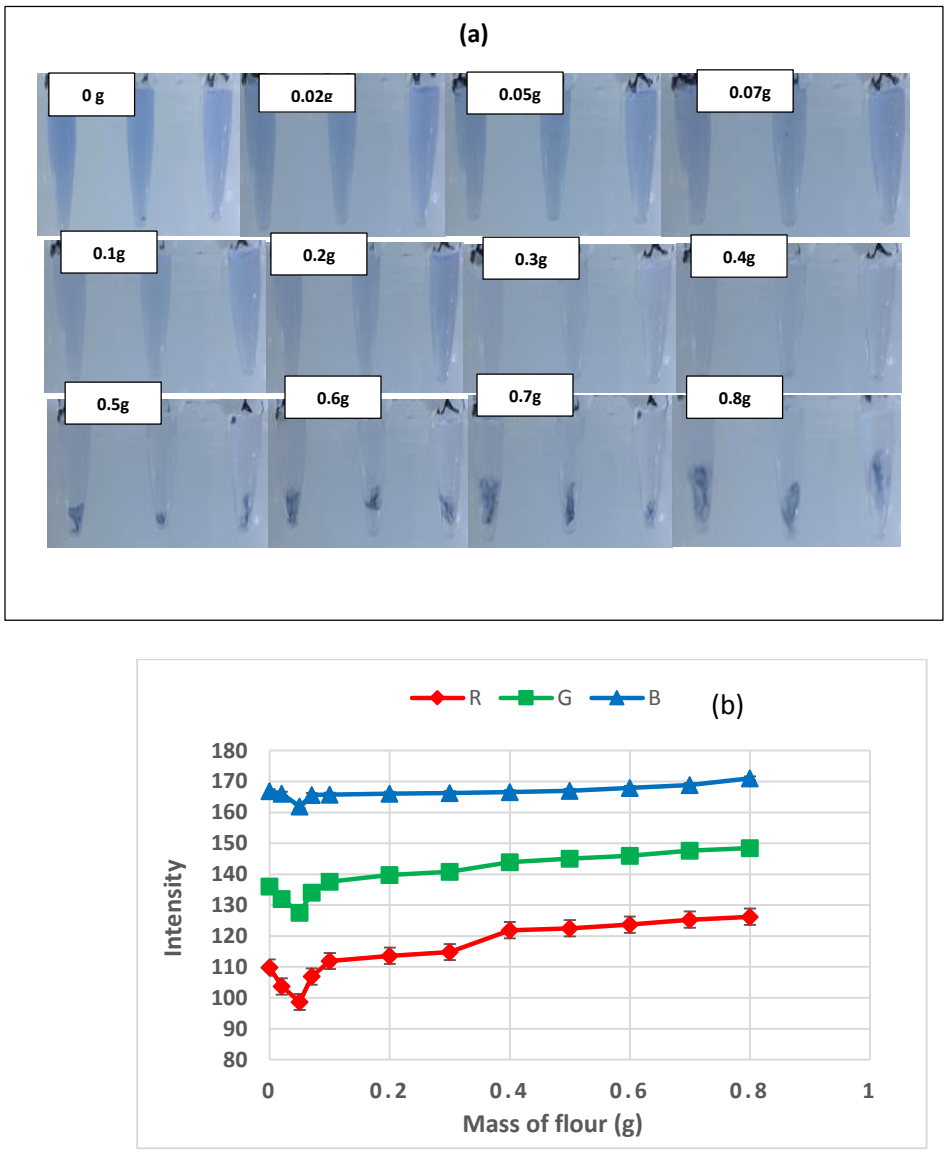

Fig 4.15 The effect of mass of flour on (a) Colorimetric product (b) RGB intensity

The film product of BF_2-curcumin and flour formed after heating was thicker at masses of flour greater than 0.4 g and could barely stick on the lid of the PCR

micro tube as required. This caused both surface of the BF_2-curcumin synthesized starch film to react with cyanide to give a reaction product at the bottom of the tube as shown in Fig 4.15(a). In view of this, masses of flour above 0.4 g could not be used. In addition, the RGB intensity initially decreased when the mass of flour was increased from 0 - 0.05 g (Fig 4.15(b)). However, the intensity increased after 0.05 g of flour. This indicated the unstabilized reaction product at excess mass of flour. Moreover, the increase in the RGB intensity after 0.05 g was also attributed to less available reagents to react with the analyte corresponding to faint blue color product. This effect was basically because, increased in mass of the flour caused an increased in density since volume of the mixture was held constant. Increased in density decreased the total reacting surface area of the reagent which in turn caused a less reaction product. Considering the effect of different masses of flour, 0.05 g was chosen and fixed as the optimum mass of flour and used for further experiment.

4.10.2 Effect of BF_2-curcumin concentration

The optimum mass of flour (0.05 mg/L) was fixed to investigate the optimum concentration of BF_2-curcumin. The concentration BF_2-curcumin was varied in the range of 0.02 - 0.8 mM. Each concentration was first tested with 1 mL of 20 mg/L CN^- solution. The effect of the reagent concentration on the colorimetric product and intensity were shown in Fig. 4.16

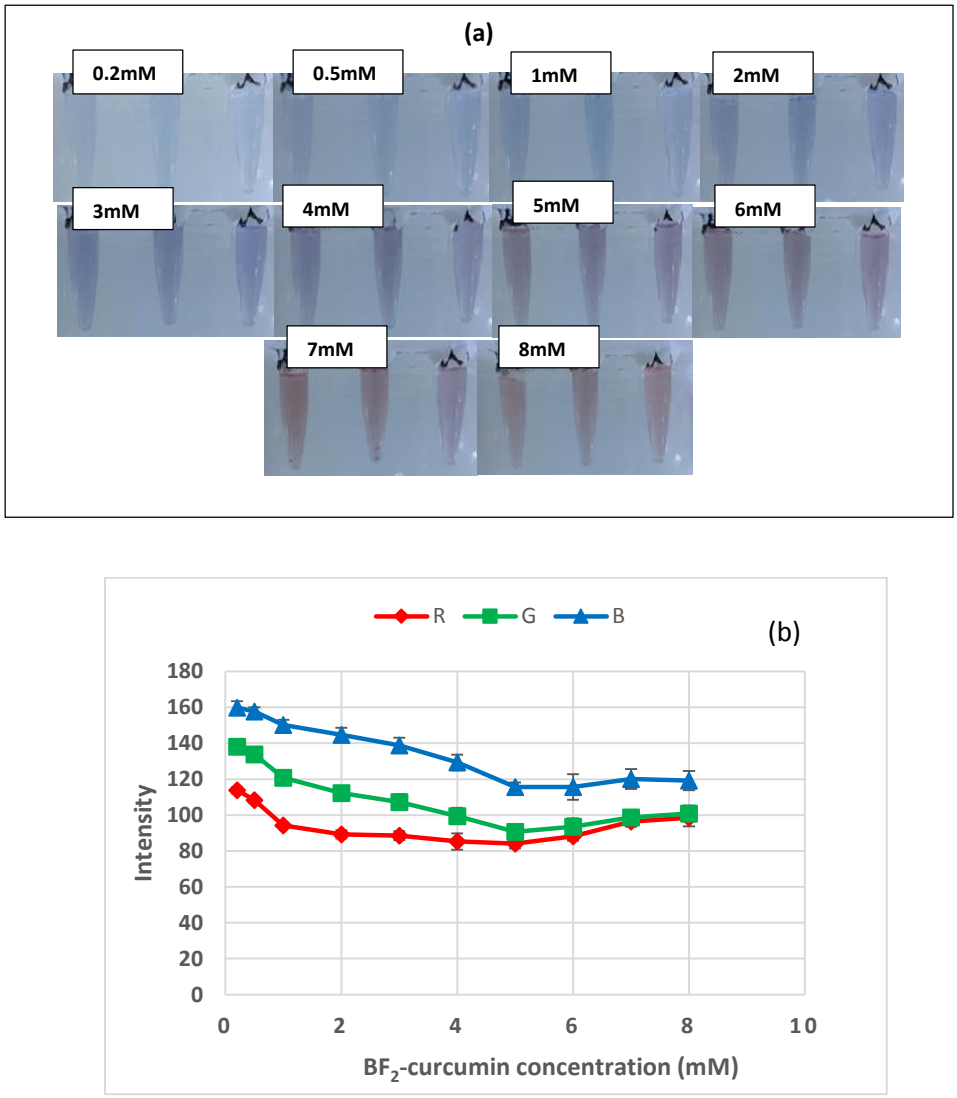

Fig 4.16 Effect BF_2-curcumin concentration on (a) Colorimetric product and (b) RGB intensity. (Conti.)

As shown in Fig. 4.16(a), the blue colored reaction product became darker as the concentration of the reagent was increased. Nevertheless, a sudden change of color from blue to brown was observed after 5 mM. The apparent change in color from blue to brown observed effect was ascribed to excess concentration of the brown reagent

which turned to dilute the solution after the complete deprotonation of BF_2-curcumin. In addition, as shown in figure 4.16(b), the RGB intensity decreased with increased BF_2-curcumin concentration. However, the intensity began to increase at concentrations above 5 mM. This was also ascribed to the apparent change in the targeted color of the reaction product. To establish the exact optimum concentration, BF_2-curcumin reagent (2 – 5 mM) were subsequently tested against low cyanide concentration *i.e.* 10 and 5 mg/L CN^-. The results are shown in Fig. 4.16 (c) and (d).

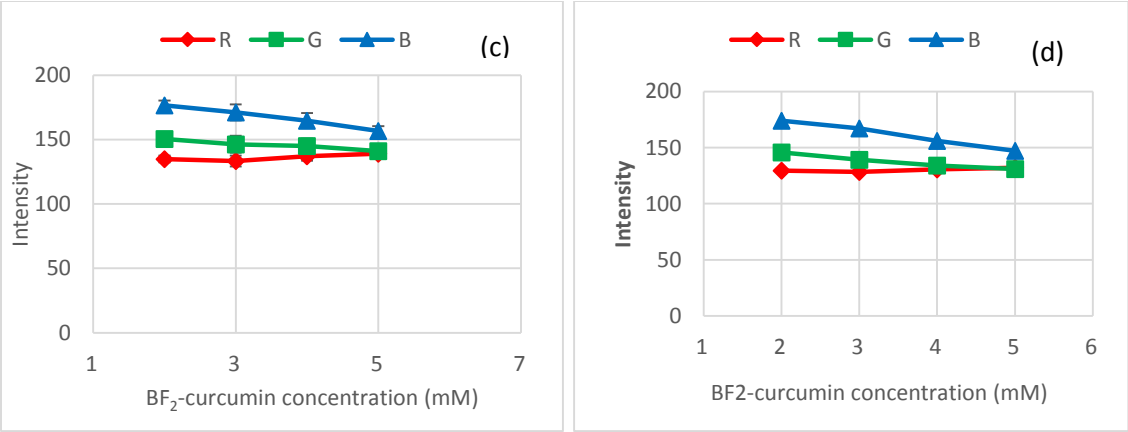

Fig 4.16 Relationship between BF_2-curcumin concentration and RGB intensity (c) 10 mg/L (d) 5 mg/L. (Conti.)

It was observed that, 5 mM of BF_2-curcumin gave the least intensity with both concentration corresponding to the highest reaction product. In addition, the results showed the optimum of 5 mM was enough to detect low concentration of cyanide, even 5 mg/L. In view of this observation, 5 mM was chosen as the optimum reagent concentration for subsequent experiment.

4.10.3 Effect of temperature in oven

The temperature at which the sensor was kept in an oven to obtain the dry product was varied between the ranges of 50 - 75 °C. The results were shown in Fig 4.17.

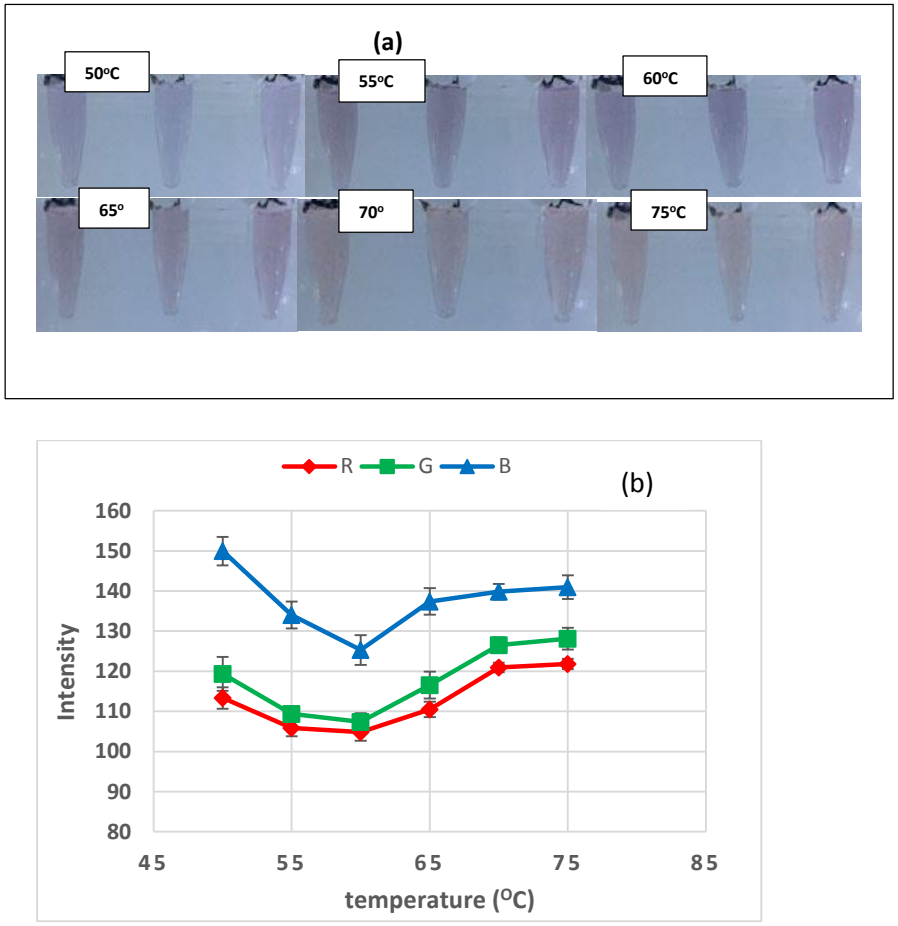

Fig 4.17 Relationship between temperature in oven and (a) colorimetric product (b) RGB intensity.

As shown in Fig. 4.17(a), the blue reaction product became darker as the temperature in the oven was increased from 50 to 60 °C. The darkest color was observed at 60 °C. However, the color began to blanch after 60 °C. In addition, the least

RGB intensity which corresponded to the highest reaction product was observed at 60 °C Fig 4.17(b). This indicated the film lost its sensoring property when temperature was higher than 60 °C. Both results from the colorimetric product and RGB intensity showed that 60 °C was the optimum oven temperature to change the solution to the film product.

4.10.4 Effect of reaction time

After the addition of CN^- solution to the test kit, the solution was shaken and left to settle. The solution rapidly turned to blue and its intensity was measured. Reaction time was varied from 1 – 30 min.

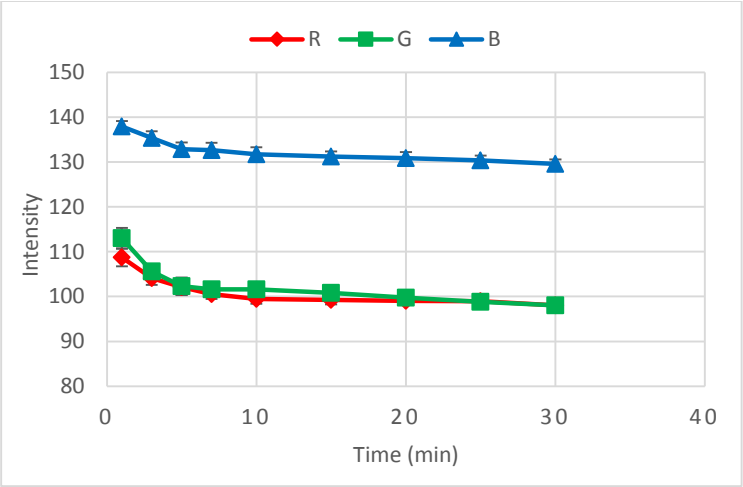

Fig. 4.18 Effect of reaction time on RGB intensity

The RGB values gradually decreased with time. However, as shown in Fig. 4.18, there was significantly no effect of reaction time on the color intensity over 5 min. These referred to the high reaction rate between CN^- and BF_2-curcumim. Based on this observation, RGB intensity was noticed in the time frame of 5 after reaction start.

4.10.5 Effect of time spent in oven

During the preliminary test it was observed that the solution in the reaction tube was still not dried up at times below 30 minutes. The effect on heating time was therefore varied between 30 - 210 minutes. The blue color product became darker with time but however began to fade after 90 minutes as shown in figure 4.19(a).

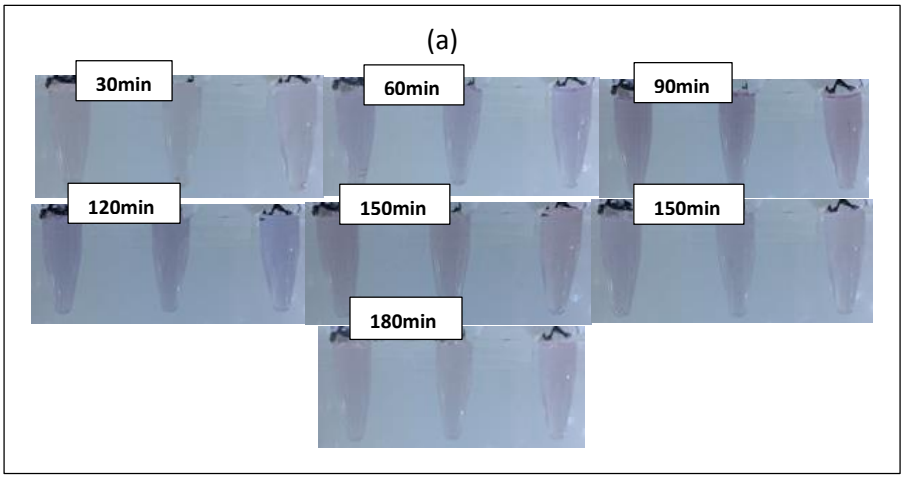

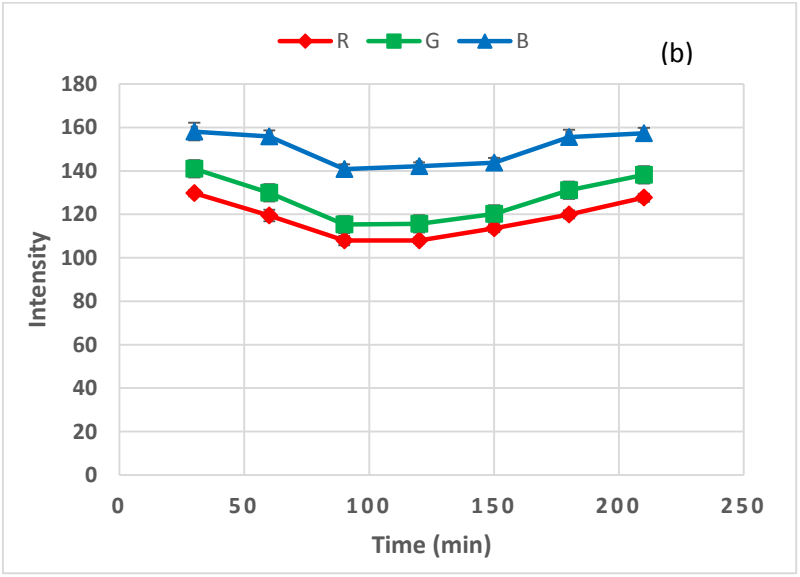

Fig 4.19 Effect of heating time on (a) colorimetric product (b) RGB intensity.

The RGB values decreased from the 30th minutes to the 90th minutes when it began to increase. The increment was apparent after the 120th min (Fig. 19(b)). Sampling time in the oven was therefore fixed at 90 min since it gave the least RGB intensity which corresponds to the highest reaction product.

4.10.6 Effect of volume of solution in the reaction tube

Obviously, the volume of BF_2-curcumin in tube reflected the amount of reactant, the effect of the volume of BF_2-curcumin synthesized starch solution in the micro tube on the intensity was therefore explored. This was to obtain the exact volume which will yield the highest reaction product. The results are presented in Fig. 4.20.

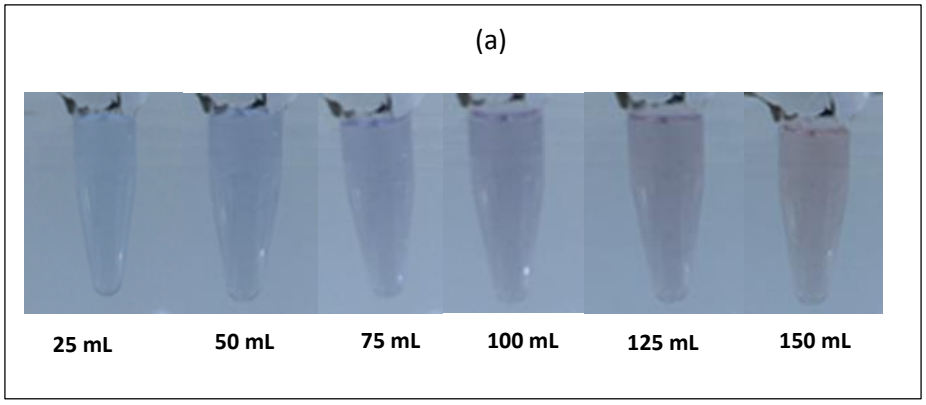

Fig. 4.20 Effect of volume of BF_2-curcumin synthesized starch solution in tube on (a) colorimetric product and (b) RGB intensity.

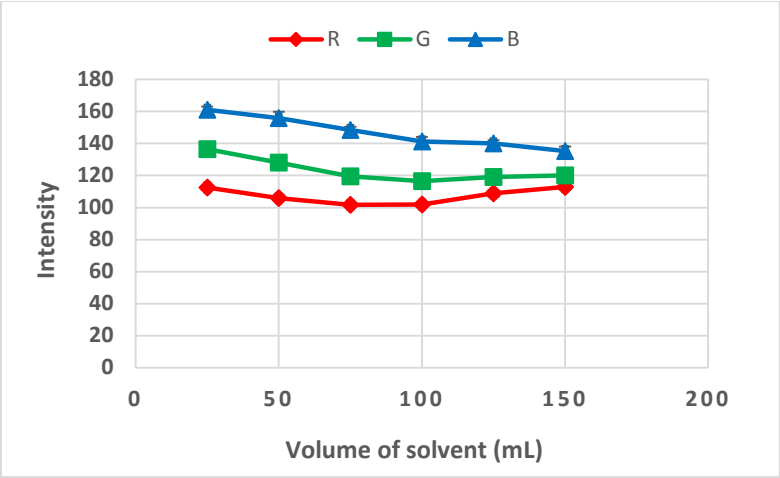

Fig. 4.20 Effect of volume of BF_2-curcumin synthesized starch solution in tube on (a) colorimetric product and (b) RGB intensity. (Conti.)

The blue product gradually became intense as the volume of the solution was increased. However, there was a significant change of color from blue to brown after 100 mL of the solution Fig. 4.20(a) corresponding to a rise in RGB intensity values. RGB intensity gradually decreased from 25 mL to 100 mL as shown in Fig 4.19. A clear rise in the intensity was observed after 100 mL. The rise in the intensity become obvious as the volume was increased from 125 and 150 mL. This observation was ascribed to the excess reagent which turned to dilute the intensity of the colorimetric product. The volume of the solution was therefore fixed at 100 mL since it gave the least intensity.

4.10.7 Effect of pH of sample

The pH effect on the colorimetric product and the RGB intensity values was investigated by first testing the sensor with a blank solution at different pH (5, 6, 7, 8, 9, 10, and 11). The color of the reaction products remain unchanged at pH 6 - 9 but however turned to blue at pH > 9 as shown in Fig. 4.21(a).

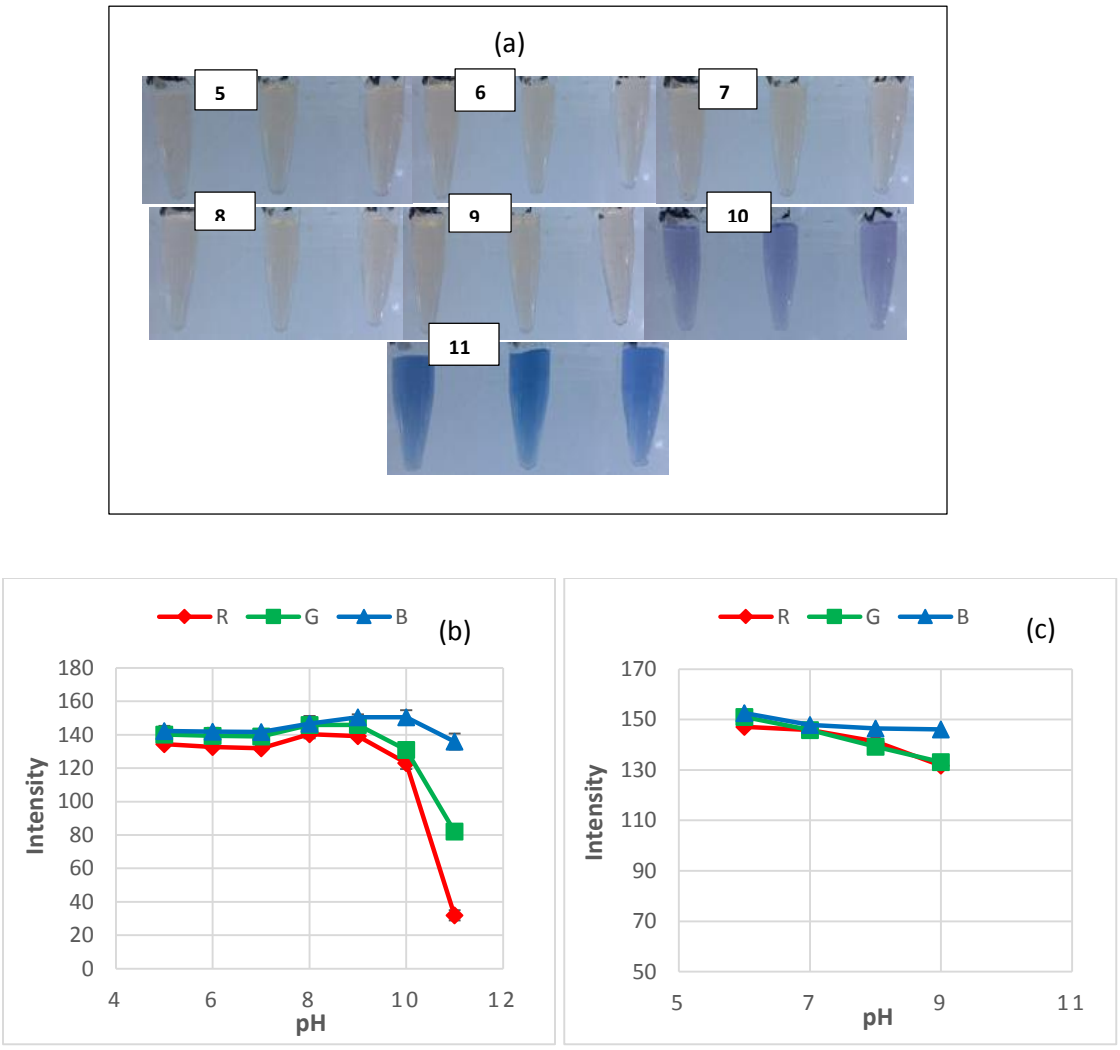

Fig 4.21 Effect of pH on (a) colorimetric product (b) RGB intensity when tested with 1mL blank sample (c) when tested with 10 mg/L cyanide.

Agreed with the results from reagent part, the measured intensity (I_R, I_G, I_B) from the blank test remained significantly unchanged over the range of 5 – 7 Fig. 4.21(a). There was a sudden rise in the intensity over the range of 7 - 9. However, the RGB intensity began to fall after pH 9 corresponding to the formation of a blue color product Fig 4.21(a). The fall was very distinct at pH 10 and 11. The sudden fall in intensity at pH > 9 was ascribed to an increased in light absorption of blank blue product which resulted in a

decrease in reflectance. This observation indicated the unstability of BF_2-curcumin extract at pH > 9. The pH 6, 7, 8 and 9 which did not show any color were subsequently tested with 10 mg/L CN^- solution Fig. 4.21(c). As presented in Fig 4.21(c), the least RGB intensity was observed at pH 9 which signifies the highest reaction product. The sample pH was therefore fixed at 9 for the subsequent experiments.

The optimum conditions for the synthesis and reaction of BF_2-curcumin synthesized starch film with cyanide were found to be 0.05 g of flour, 5 mM BF_2-curcumin, 60° C oven temperature, 5 min of reaction time, 90 min of time spent in the oven, 100 µL of solution in the PCR tube and sample pH of 9.

Images from scanning electron spectroscopy of the blank and BF_2-curcumin synthesized starch film are shown in Fig. 4.22.

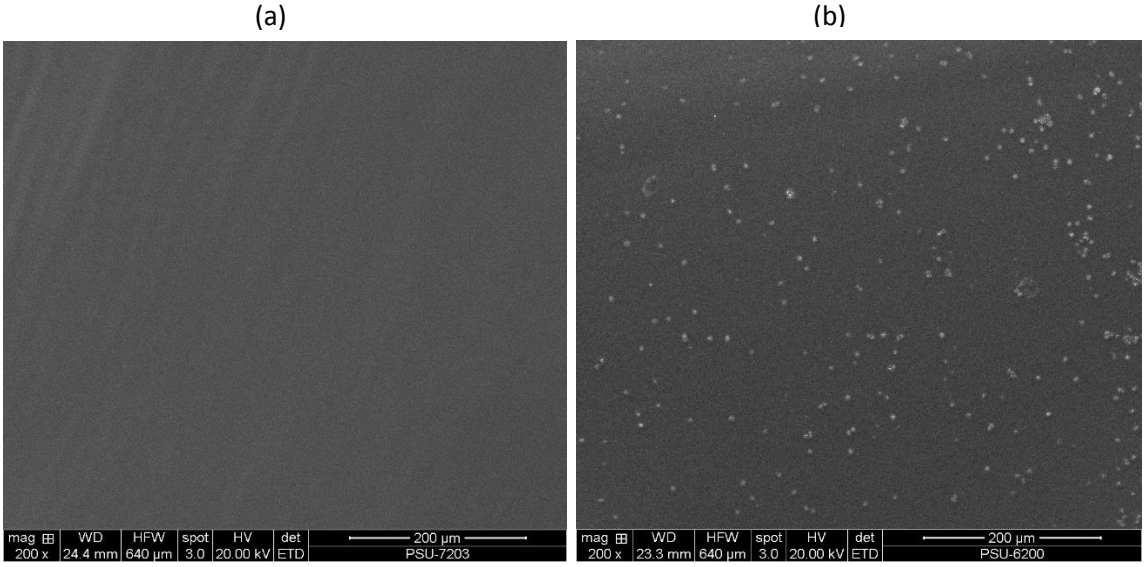

Fig 4.22 Image from scanning electron microscopy (SEM) of (a) starch film (blank) and (b) BF_2-curcumin synthesized starch film.

The blank starch film showed a smooth surface without any particles Fig. 4.22(a). The curcumin was identified to be the white particles anchored in the polymer.

It is these particles that react with cyanide to produce the blue color product. The polymer showed a good compatibility with the curcumin particles.

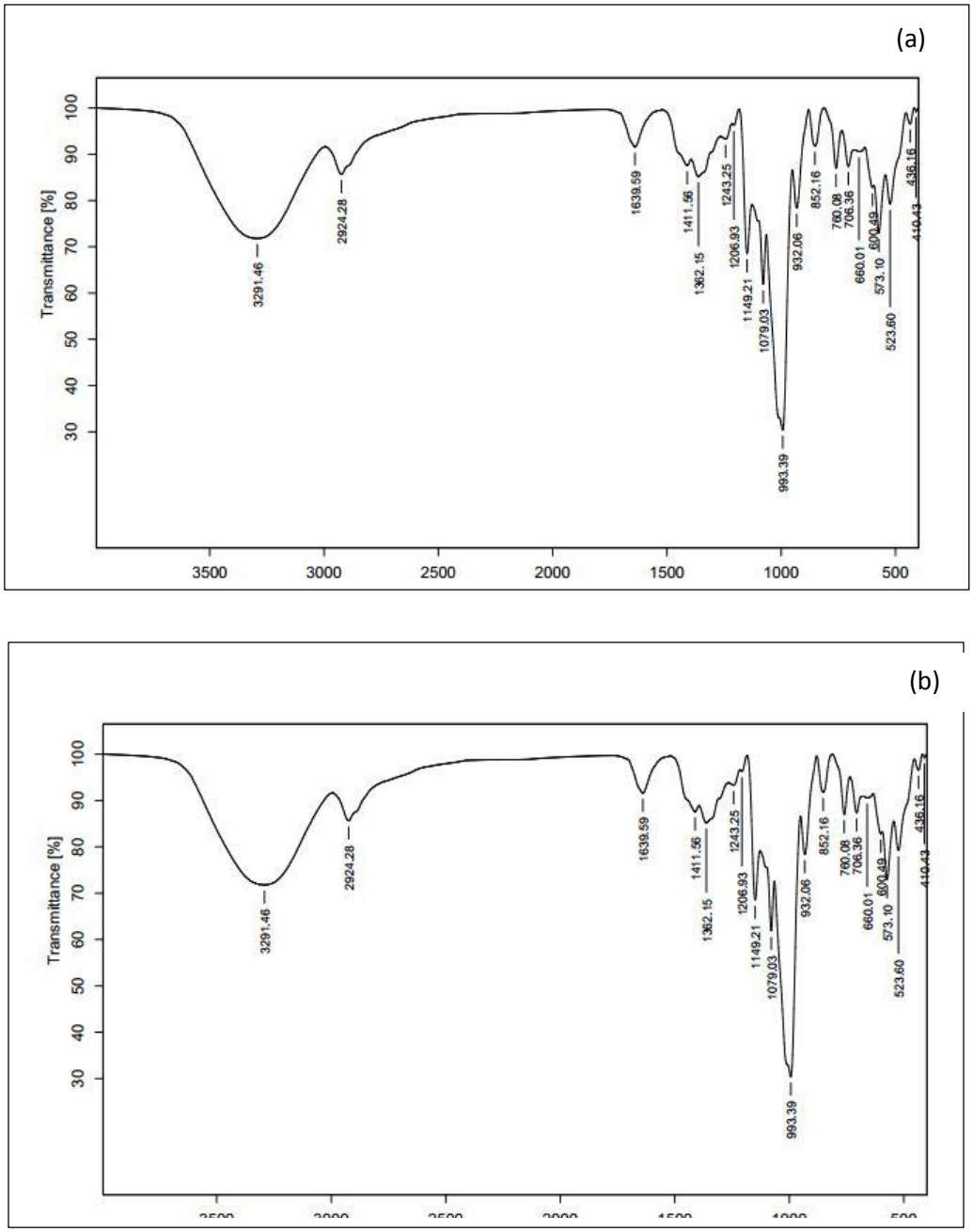

Fig 4.23 FTIR spectrum of (a) blank starch film and (b) BF_2-curcumin reagent anchored in the molecular structure of the starch film.

4.11 Colorimetric reaction of BF_2-curcumin synthesized starch film and CN^-

A colorimetric test of CN^- with the sensor produced a faint brown-blue color product. The brown-blue color gradually turned into blue and became darker as the concentration of CN^- solution was increased (Fig. 24).

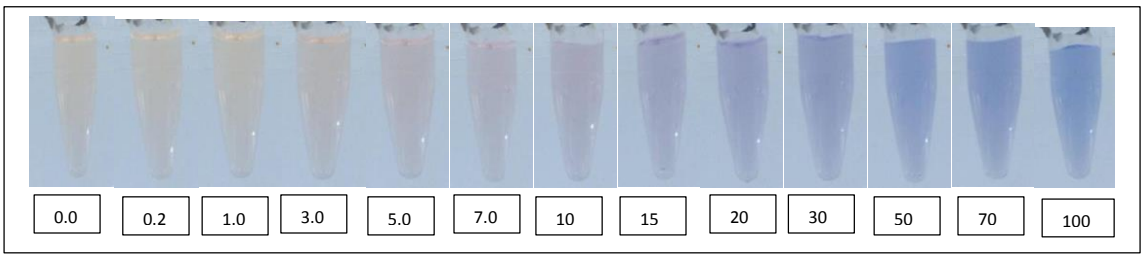

Fig 4.24 Colorimetric products obtained from reaction with various concentrations of cyanide solution (0.2 to 100 mg/L).

4.12 Individual RGB intensity analyzed by BF_2-curcumin synthesized starch film

The quantification of cyanide using BF_2-synthesized starch film was achieved by digital image colorimetric as previously described in 4.3. Digital image of the blue complex produced by CN^- were captured and their intensities measured. The intensity of the blue channel was the highest among the three color channels followed by green and red respectively. This difference became clearer as the concentration of cyanide was increased and presented as a dark colored product (Fig 4.24). The blue channel showing the highest intensity indicated that, the sample reflected more light in the blue region. In addition, the highest sensitivity was observed by the green color with slope of 1.663 a.u. L/mg. The red color channel was next to the green color in sensitivity followed by the blue with slopes of 1.3398 and 0.8624 a.u. L/mg, respectively (Fig 4.25(b)).

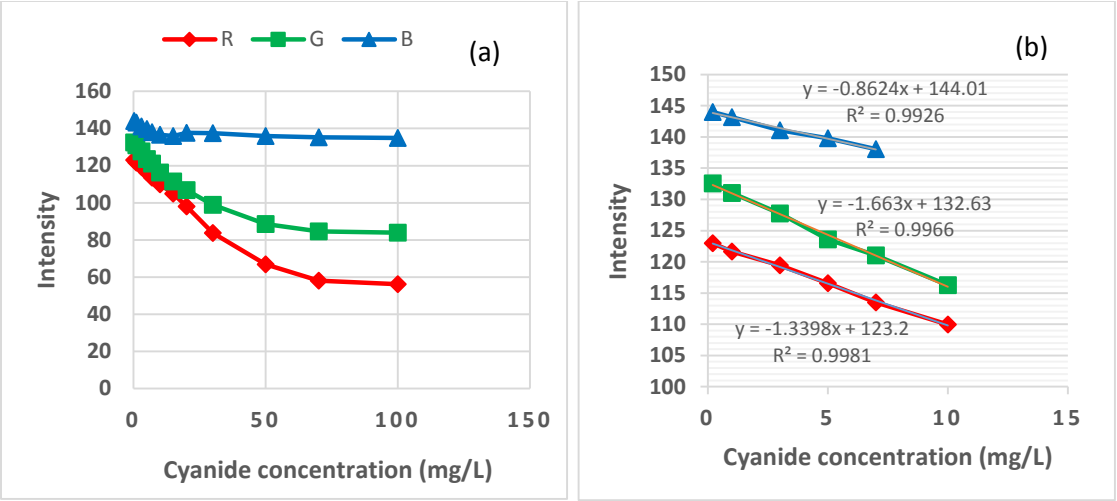

Fig 4.25 Relationship between cyanide concentration and (a) individual RGB intensity, (b) RGB intensity linear range (0.2-7 mg/L)

As presented in Fig. 25(b), the linear range was observed in the range of 0.2 to 10 mg/L for the red and green color channel. However, it was observed within the range of 0.2 to 7 mg/L for the blue color channel.

4.13 Individual RGB absorbance

The absorbance of the reaction products were also investigated by calculating the molecular absorption of the colorimetric product using equation 1. The red channel revealed the highest level of absorbance followed by green and blue channel respectively. This observation corresponded to the inverse relationship between RGB intensity and RGB absorbance. The calculated RGB absorbance increased with increased cyanide concentrations. Likewise to the sensitivity of the individual color channel of the RGB intensity, the highest sensitivity was observed at the green color channel followed by red and blues respectively as shown in Fig. 4.26(b).

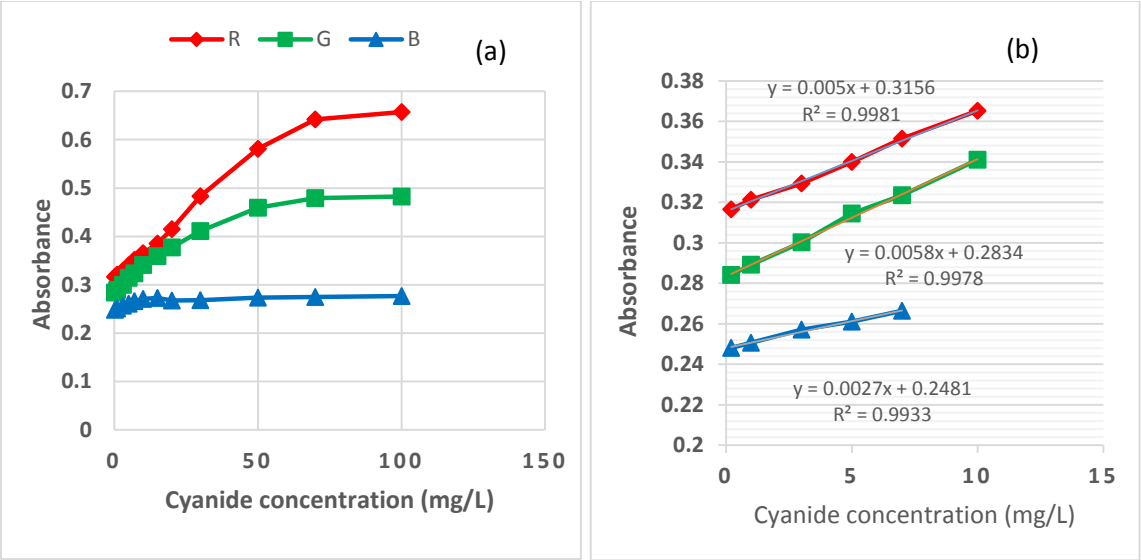

Fig 4.26 Relationship between cyanide concentration and (a) individual RGB absorbance (b) RGB absorbance linear range.

4.14 Total RGB values

As previously describe in 3.4, the total RGB values *i.e.* total intensity and absorbance were considered since they will provide some more comprehensive information to that of the individual values. The relation between total RGB values and cyanide concentration are presented in Fig. 4.27.

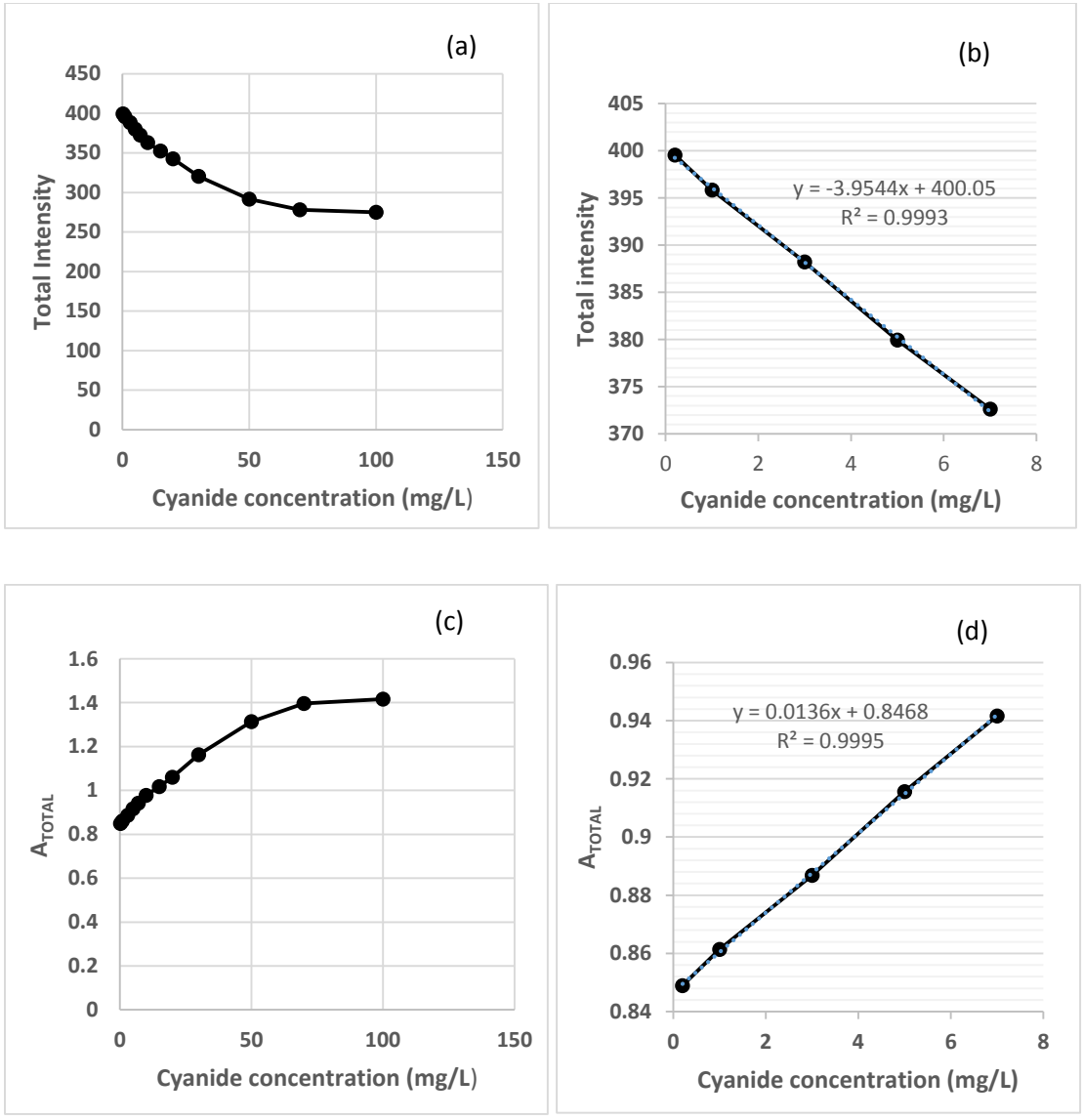

Fig 4.27 Relationship between total RGB values and cyanide ion concentration (a) I_{TOTAL} (b) linear range for I_{TOTAL}, (c) A_{TOTAL} (d) linear range for A_{TOTAL}.

As shown in Fig. 4.27 (b) and (d), the linear ranges of the total RGB values were the same as that of the individual values but provided higher overall intensity.

4.15 Blank subtracted RGB values

The relationship between cyanide concentration and RGB values of the colored product, from which the RGB value of the blank was subtracted was investigated. Both individual and total intensity and absorbance were studied.

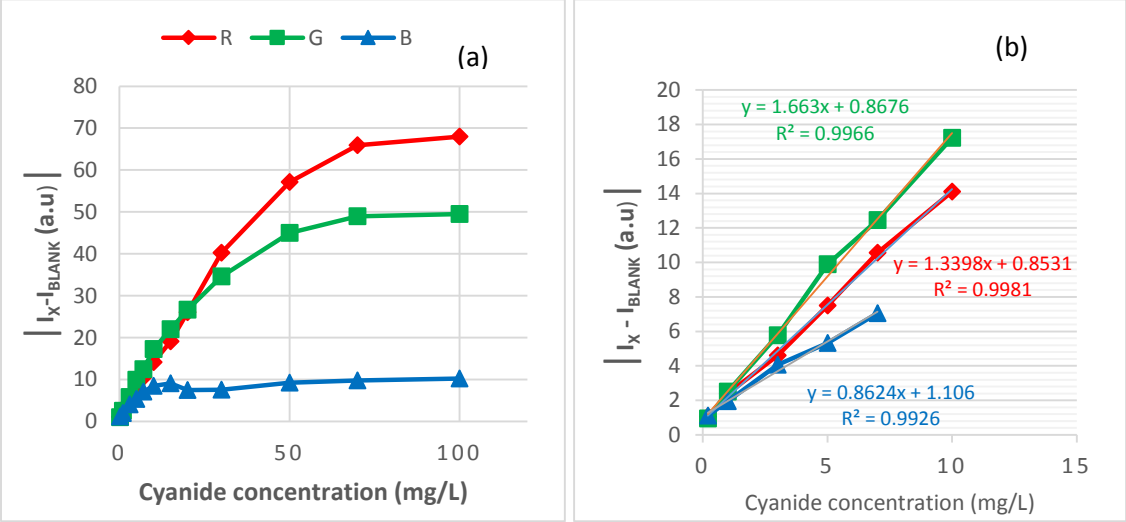

Fig 4.28 Relationship between blank subtracted RGB values and cyanide concentration for (a) individual intensity, (b) linear range for blank subtracted individual intensity, (c) individual absorbance and (d) linear range for blank subtracted individual absorbance.

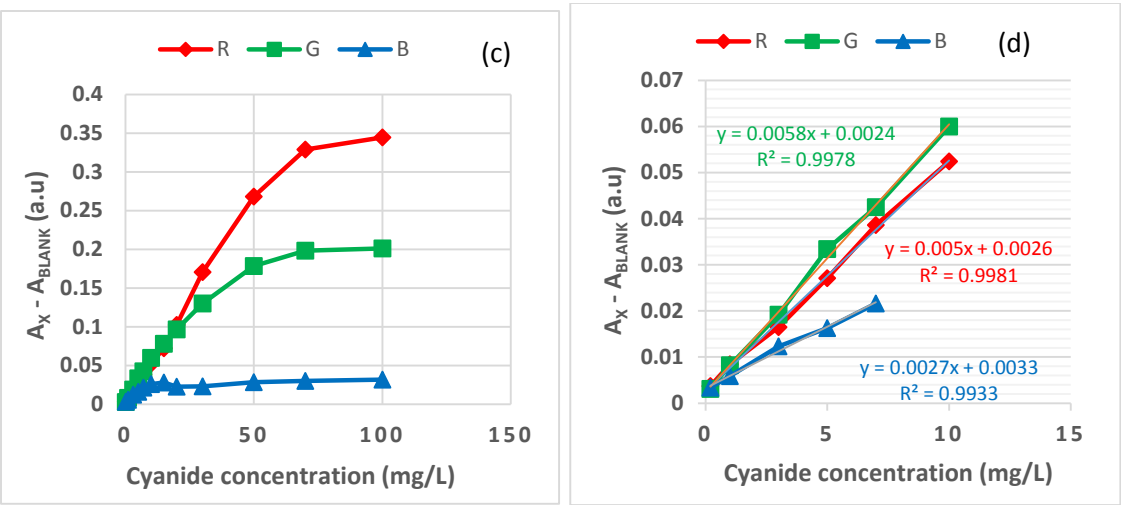

Fig 4.28 Relationship between blank subtracted RGB values and cyanide concentration for (a) individual intensity, (b) linear range for blank subtracted individual intensity, (c) individual absorbance and (d) linear range for blank subtracted individual absorbance. (Conti.)

When the RGB values of the blank were subtracted, the intensity decreased with increasing cyanide concentration whereas the absorbance increased with increasing cyanide concentration. This observation did not show any difference with the RGB values without the blank subtraction. The green color channel showed the highest sensitivity imitating the results when the individual RGB values were considered. The total blank subtraction from the total RGB intensity and absorbance were also considered as mentioned in 3.5. The results are presented in Fig 4.29

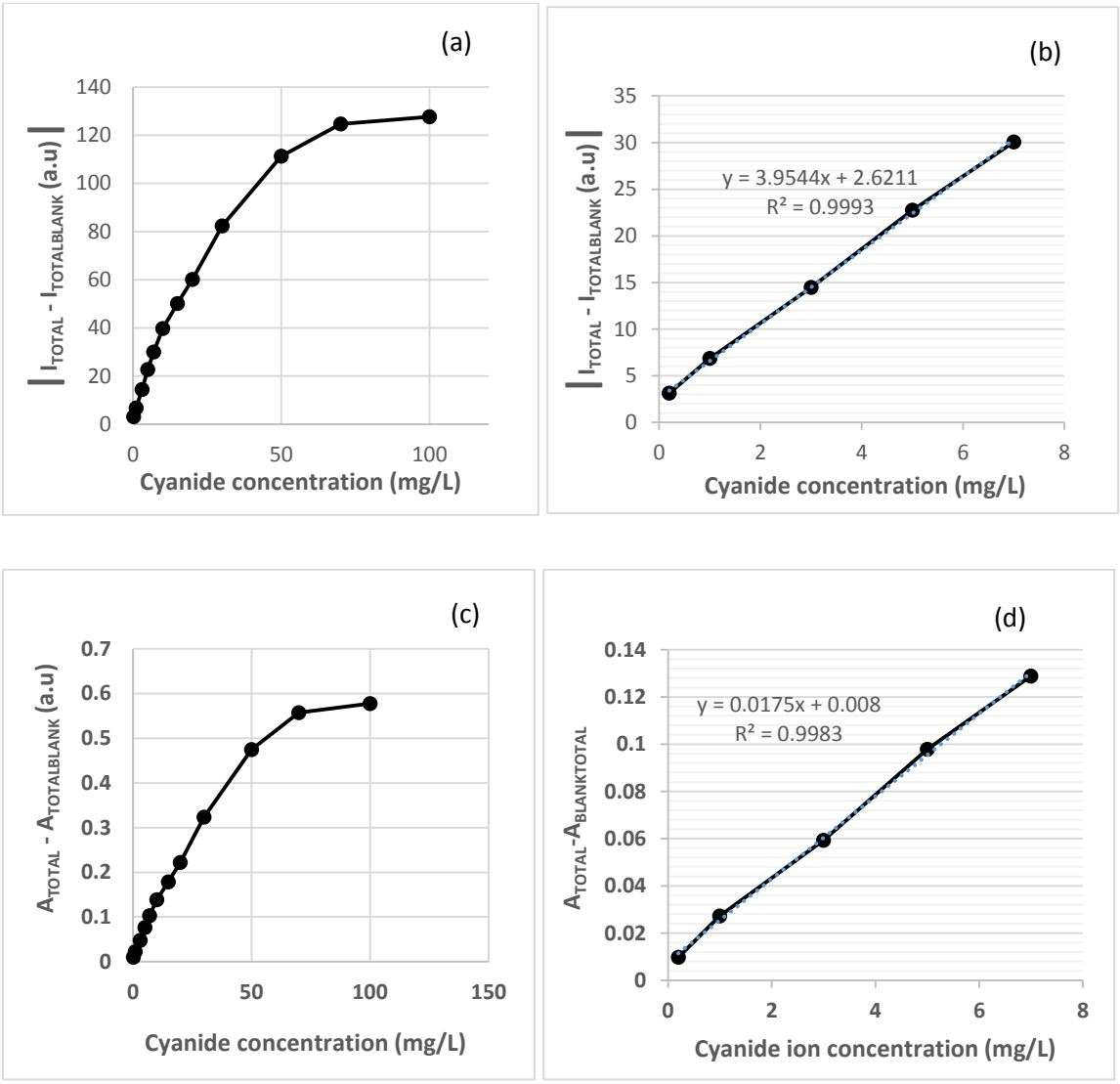

Fig 4.29 Relationship between blank subtracted RGB values and cyanide ion concentration (a) total intensity (b) linear range of total intensity (c) total absorbance (d) linear range of total absorbance.

The blank subtraction from the total RGB intensity value gave a higher sensitivity as compared to the blank subtraction of the individual intensity (Fig. 4.27 (b) and (d)). However, the blank subtraction of the RGB absorbance gave less sensitivity to that of the individual absorbance.

4.16 Analytical performances and method validation

The linear range, calibration equation and linearity of the BF_2-curcumin synthesized starch film sensor are summarized in table 4, while other analytical performances, i.e. precision and accuracy are shown in table 5.

Table 4.4 Calibration equation, sensitivity, linear range and for correlation coefficient for the detection of cyanide by the sensor

Relationships	Linear range (mg/L)	Calibration equation	R^2
I_R and C	0.2-10	y = (-1.340 ± 0.03)x + (123.2 ± 0.1)	0.9981
I_G and C	0.2-10	y = (-1.663 ± 0.05)x + (132.63 ± 1.8)	0.9966
I_B and C	0.2-7	y = (-0.862 ± 0.03)x + (144.01 ± 0.4)	0.9926
A_R and C	0.2-10	y = (0.005 ± 0.0001)x + (0.316± 0.004)	0.9981
A_G and C	0.2-10	y = (0.006 ± 0.0002)x + (0.283 ± 0.006)	0.9978
A_B and C	0.2-7	y = (0.003 ± 0.00009)x + (0.248 ± 0.001)	0.9933
I_{TOTAL} and C	0.2-7	y = (-3.954 ± 0.1)x + (400.05 ± 2.5)	0.9993
A_{TOTAL} and C	0.2-7	y = (0.014± 00.0002)x + (0.847 ± 0.003)	0.9995
I_R - I_{Rblank} and C	0.2-10	y = (-1.340 ± 0.04)x - (0.853 ± 1.3)	0.9981
I_G - I_{Gblank} and C	0.2-10	y = (-1.663 ± 0.06)x - (0.868 ± 2.05)	0.9966
I_B - I_{Bblank} and C	0.2-7	y = (-0.862 ± 0.03)x - (1.106 ± 0.4)	0.9926
A_R - A_{Rblank} and C	0.2-10	y = (0.005 ± 0.0001)x + (0.0026 ± 0.004)	0.9981
A_G - A_{Gblank} and C	0.2-10	y = (0.006 ± 0.0002)x + (0.0024 ± 0.006)	0.9978
A_B - A_{Bblank} and C	0.2-7	y = (0.003 ± 0.00009)x + (0.0033 ± 0.001)	0.9933
(I_R -I_{Rblank}) + (I_G - I_{Gblank}) + (I_B - I_{Bblank}) and C	0.2-7	y = (-3.954 ± 0.06)x - (2.6211 ± 0.2)	0.9993
(A_R -A_{Rblank}) + (A_G - A_{Gblank}) + (A_B -A_{Bblank}) and C	0.2-7	y = (0.014 ± 0.0002)x + (0.008 ± 0.0007)	0.9995

Table 4.5 Limit of detection, accuracy and precision of BF_2-curcumin synthesized starch film

Relationships	LOD (mg/L)	Accuracy			Precision (%RSD)	
		Known (mg/L)	Measured (mg/L)	%Relative error	Intra-day	Inter-day
I_R and C	0.43 ± 0.007	4	4.049	1.176	0.74-1.10	0.61-1.12
I_G and C	0.60 ± 0.020	4	3.887	2.836	0.10-1.17	0.82-1.25
I_B and C	0.84 ± 0.029	4	4.195	4.880	0.31-0.48	0.39-0.40
A_R and C	0.55 ± 0.012	4	3.975	0.616	1.11-1.48	0.77-1.66
A_G and C	0.58 ± 0.018	4	3.827	4.330	1.88-2.28	1.33-2.20
A_B and C	0.82 ± 0.028	4	3.987	0.335	1.09-1.70	1.18-1.21
I_{TOTAL} and C	0.51 ± 0.015	4	3.946	1.341	0.50-0.78	0.24-0.78
A_{TOTAL} and C	0.21 ± 0.003	4	3.907	2.323	1.15-1.37	0.43-1.51
I_R - I_{Rblank} and C	0.34 ± 0.010	4	4.049	1.222	2.93-3.33	1.74-3.89
I_G - I_{Gblank} and C	0.68 ± 0.025	4	3.888	2.800	4.24-6.00	2.64-6.36
I_B - I_{Bblank} and C	0.84 ± 0.029	4	4.064	1.609	6.24-13.47	4.69-6.52
A_R - A_{Rblank} and C	0.55 ± 0.012	4	3.991	0.236	3.10-3.66	2.17-4.36
A_G - A_{Gblank} and C	0.57 ± 0.018	4	3.817	4.583	4.64-6.38	2.98-6.90
A_B - A_{Bblank} and C	0.84 ± 0.029	4	3.972	0.701	6.37-13.52	4.75-6.57
$(I_R - I_{Rblank}) + (I_G - I_{Gblank}) + (I_B - I_{Bblank})$ and C	0.25 ± 0.004	4	3.945	1.368	3.19-4.06	1.32-4.29
$(A_R - A_{Rblank}) + (A_G - A_{Gblank}) + (A_B - A_{Bblank})$ and C	0.21 ± 0.003	4	3.905	2.364	3.57-4.33	1.39-4.73

The limit of detection calculated using the standard method (LOD = y_B + $3S_B$ where y_B is the intercept of the calibration curve and S_B is the standard deviation of blank) were in a range of 0.21 ± 0.003 to 0.84 ± 0.029 mg/L. Accuracy evaluated as %relative error as described in 4.6 was generated by analyzing a known concentration of cyanide standard (x_{Known} = 4 mg/L) and quantified using external calibration. A relative error of 0.236 to 4.195% was obtained indicating good accuracy of analysis. The precision in terms of %RSD from 3 repetition of the analysis of cyanide (20 mg/L) within the same day (intra-day), were in the range of 0.65 to 2.51%RSD for the intensity. The calculated absorbance precision ranged from 0.83 to 2.81%. When the analysis were performed over three days, the precision ranged from 1.15 to 2.97% and 1.85 to 3.44 for the intensity and calculated absorbance respectively. The total RGB values also gave good precision but the blank subtracted RGB values however gave poor precisions conforming to the results obtained in the investigation of the reagent 4.6.

4.17 Stability of BF_2-curcumin synthesized starch film

As previously described in 4.7, several BF_2-curcumin synthesized starch film were prepared at the same time to investigate the stability sensor. The regent were split into two groups with one part stored in a desiccator whereas the other part stored under room temperature. Three test kits were removed from each part for cyanide detection within a period of 1, 3, 7, 14, 28, 56 and 84 days. The RGB intensities of the sensors stored under room temperature altered by 3.297%, 8.727% and 4.986% (Fig. 4.30(a)) respectively throughout the experimental period (1 - 84 days) with reference to the least intensity recorded on the first day which corresponds the highest reaction product (Fig. 4.28). The test kits stored in a desiccator also altered by 11.478%, 5.891% and 5.799% respectively (Fig. 4.30(b)).

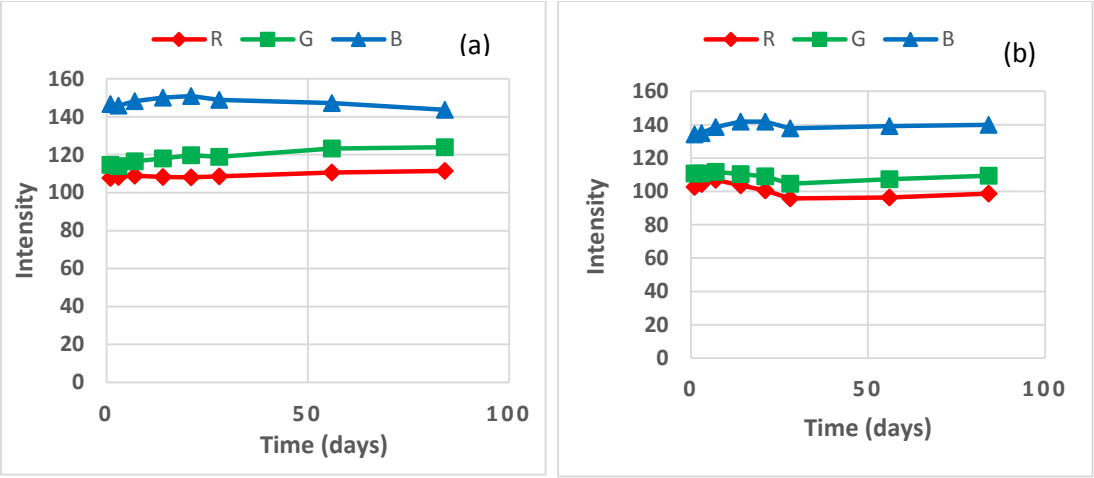

Fig 4.30 Stability of BF_2-curcumin synthesized starch sensor stored under (a) room temperature (b) desiccator.

4.18 Interference

The sensing ability of the BF_2-curcumin synthesized starch sensor was examined by Cl^-, NO_3^-, SO_4^{2-}, and PO_4^{3-}. The results are presented in Fig. 4.31.

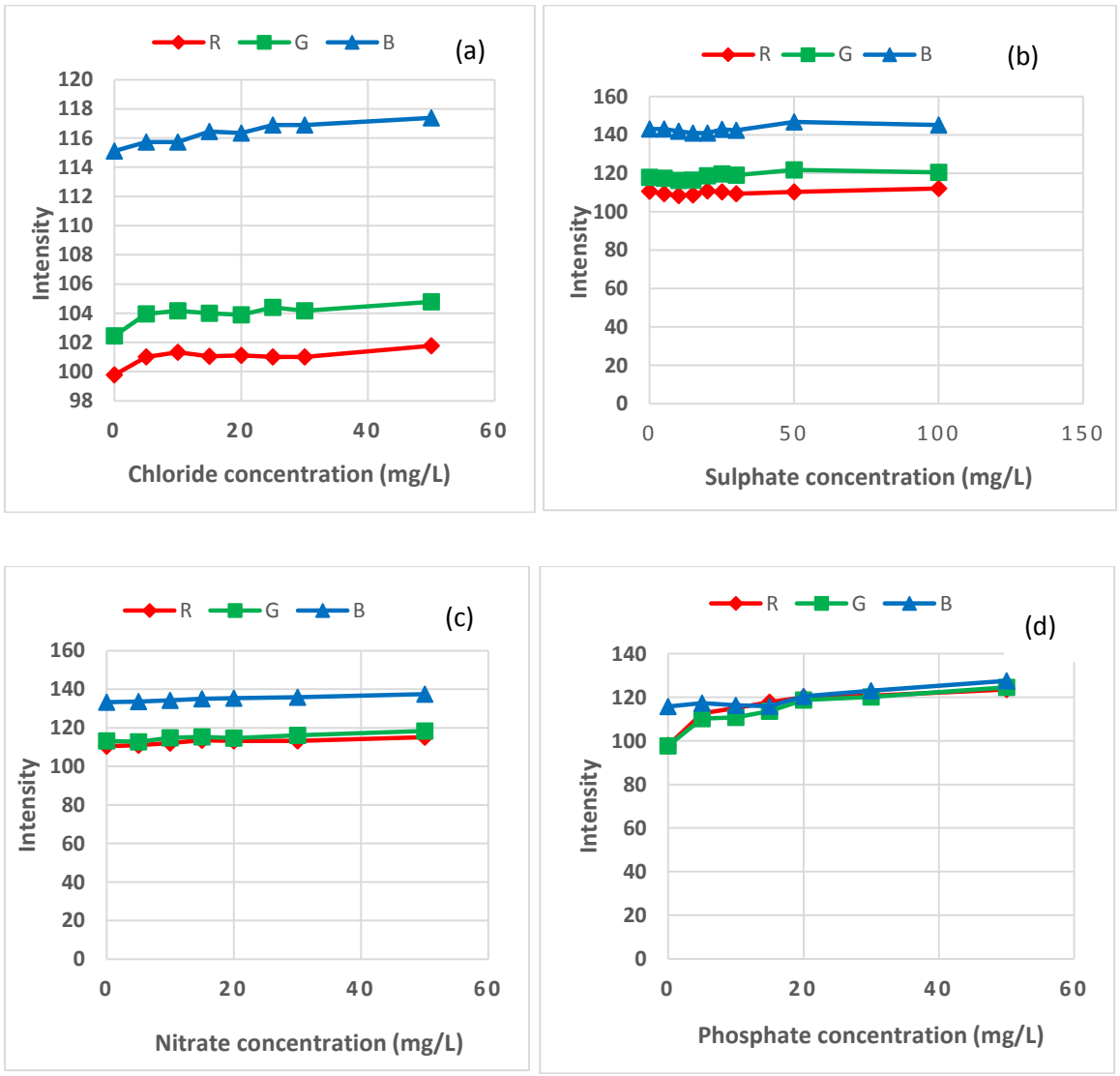

Fig 4.31 Effect of interfering ions on the RGB intensity of 20 mg/L CN^- solution (a) chloride (b) nitrate (c) sulfate (d) phosphate

Addition of different concentrations of chloride (0 - 50 mg/L) anions changed the RGB intensity values of 20 mg/L cyanide solution by 2.001%, 2.278%, and 1.979% respectively (Fig. 4.29(a)). Sulfate anions influenced the selectivity of 20 mg/L cyanide solution by altering the RGB intensity values by 3.330%, 4.732% and 4.101% respectively (Fig. 4.29(b)). The effect of nitrate on cyanide selectivity was also considered. The nitrate anions altered the RGB intensity values by 4.171%, 4.978% and 3.125% respectively (Fig. 4.29(c)). The RGB intensity values of the cyanide solution was disturbed by phosphate by 25.722%, 26.77% and 11.78% respectively.

4.19 Quantification of CN^- concentration in real sample

4.9.1 Quantification of CN^- concentration in real sample by sensor

By the same approach in 4.9.1, Water samples obtained from the abandoned tin mine site was tested with the developed BF_2-curcumin synthesized starch sensor. Ones again the RGB intensity value of the blank (reagent in DI water) was measured and subsequently substituted in each calibration equation as y. The measured RGB intensity of each concentration was plotted against their respective concentrations concentration (0.2, 0.4, 0.6, 0.8, and 1.0 mg/L) as presented in Fig. 4.32.

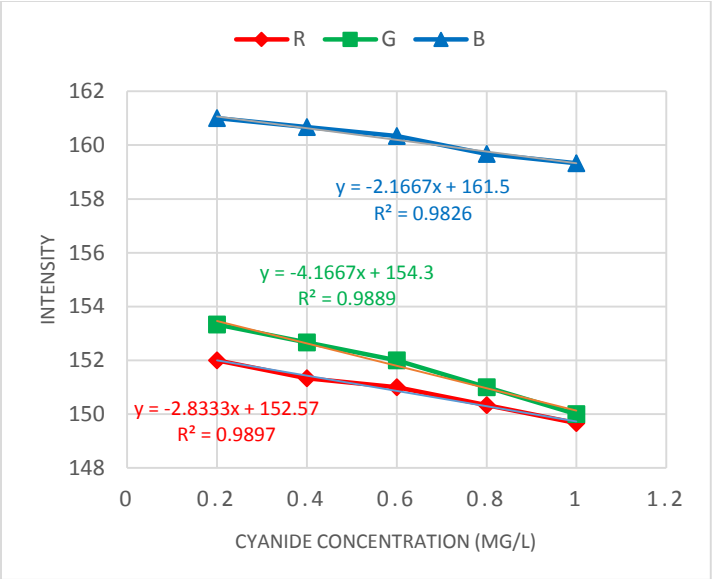

Fig 4.32 Relationship between RGB intensity and cyanide concentration from real sample using BF_2-curcumin synthesized starch film.

The results obtained by each color channel from the linear range are presented in table 4.6. It was observed that, the green and blue color gave similar concentration of cyanide in the real sample.

Table 4.6 Quantification of cyanide in the real sample by BF_2-curcumin synthesized starch film.

Intensity	y= mx + c	y	m	c	calculated
R	y= -2.833x + 152.57	155.6667	-2.833	152.57	1.09
G	y= -4.1667x + 154.3	158.6667	-4.1667	154.3	1.05
B	y= -2.1667 + 161.5	162.6667	-2.1667	161.5	0.54

Chapter 5

Conclusion

An environmentally colorimetric chemical sensor to detect cyanide in water was successfully developed by synthesizing BF_2-curcumin reagent. Parameters affecting to the synthesis of the reagent and sensor were well investigated. In addition, parameters affecting the reaction product of the developed test kit and cyanide were also optimized to achieve the optimum conditions. The color of the reagent changed from orange-red to blue upon reacting with cyanide solution. The color changed could be observed within the first minute of the reaction product by the naked eye. The regent was well entrapped in the molecular structure of a polymer due to some advantages such as specific selectivity and excellent film forming property associated with polymers. Real –time Red-Green-Blue (RGB) color data of the colorimetric product from the test kits were successfully obtained using a free of charge application installed on an iPhone. A laboratory protective box was profitably employed during the measurement of RGB intensity. This aided to avoid any environmental light interference. Quantification was substantiated with known concentration standards and real sample testing confirming the accuracy of the technique. The results were comparable with that of the spectrophotometer analysis. Stability results from the reagent and sensor showed insignificant difference between the two storage conditions, *i.e.* storage under room temperature and storage in a desiccator. The test kits had the ability to be used over long period of time under both conditions. However, it was recommended that, ambient storage should be used due to the conveniences associated with it. Both BF_2-curcumin reagent BF_2-curcumin synthesized starch film show good sensing ability among ions such as Cl^-. NO^{3-}, $SO4^{2-}$ and $PO4^{3-}$. This colorimetric method showed several advantages such

as simple synthesis of reagent and sensor, economically feasible and above all, environmentally friendly. Furthermore, the methodology demonstrated has significant potential for on-site field use in rapid detection of cyanide.

Reference

Aggarwal, B. B., Shishodia, S. (2006). Molecular targets of dietary agents for prevention and therapy of cancer. Biochemical Pharmacology, 71(10): 1397-1421.

B. R. Eggins. (2002). Chemical sensor and Biosensors, John Wiley & Sons.

Bagchi, A. (2012). IOSR Journal of Environmental Science, Toxicology and Food Technology (IOSR-JESTFT) 1(3): 01-16.

Barik, A., Priyadarsini, K. I., Mohan, H. (2003). Photophysical studies on binding of curcumin to bovine serum albumins. Photochem Photobiol. 77(6): 597-603.

Baud, F.J. (2007). Cyanide: critical issues in diagnosis and treatment. Human and experimental toxicology 26: 191-201

Bhowmick, I., Boston, D. J., Higgins, R. F., Klug, C. M., Shores, M. P., and Gupta, T. (2016). Naked eye detection of cyanide in water with Co^{II} bis(terpyridine) complex. Sensors and Actuators B: Chemical, 235: 325-329

Bui, D.A. and Hauser, P.C. (2015). Absorbance detector for capillary electrophoresis based on light-emitting diodes and photodiodes for the deep-ultraviolet range. Journal of Chromatography A, 1421: 203-208

Buske, J. L. O., Nicoleti, C. R., Cavallaro, A. A., & Machado, V. G. (2015). 4-(Pyren-1-ylimino)methylphenol and its silylated derivatives as chromogenic chemosensors highly selective for fluoride or cyanide. Journal of the Brazilian Chemical society, 26, 2507-2519

Busschaert, N., Caltagirone, C., Van Rossom, W. and Gale, P.A., (2015). Applications of supramolecular anion recognition. Chemical reviews, 115(15): 8038-8155.

Byrne, L., Barker, J., Pennarum-Thomas G., Diamond, D., Edwards, S. (2000). Digital imaging as a detector for generic analytical measurement, TrAC Trends Anal. Chem. 19: 517-522.

Byrne, L., Barker, J., Pennarum-Thomas G., Diamond, D., Edwards, S. (2000). Digital imaging as a detector for generic analytical measurement, TrAC Trends Anal. Chem. 19, 517-522.

Caciano de Sena, R., Soares, M., Pereira, M.L.O., Cruz Domingues da Silva, R., Ferreira do Rosário, F. and Cajaiba da Silva, J.F. (2011). A simple method based on the application of a CCD camera as a sensor to detect low concentrations of barium sulfate in suspension. Sensors, 11(1): 864-875.

Cantrell, K., Erenas, M.M., de Orbe-Paya, I. and Capitán-Vallvey, L.F. (2009). Use of the hue parameter of the hue, saturation, value color space as a quantitative analytical parameter for bitonal optical sensors. Analytical chemistry, 82(2): 531-542.

Chaicham A, Kulchat S, Tumcharern G, Tuntulani T. (2010). Synthesis, photophysical properties, and cyanide detection in aqueous solution of BF2-curcumin dyes. Tetrahedron, 66: 6217-6223.

Chamjagali, M, A., and Amin, A, H. (2011). Development of a simple and inexpensive optical absorption one-shot sensor membrane for detection and determination of cyanide ions in water samples. Chinese chemical society, 58: 118-125.

Chen X., Zhou Y., Peng X., Yoon J. (2010) Fluorescent and colorimetric probes for detection of thiols, Chem. Soc. Rev. 39, 2120-2135.

Chen, K.Y. and Lin, W.C. (2015). A simple 7-azaindole-based ratiometric fluorescent sensor for detection of cyanide in aqueous media. Dyes and Pigments, 123: 1-7.

Choodum A., Daeid, N. N. (2011). Rapid and semi-quantitative presumptive test for opiate drugs, Talanta 86: 284-292

Choodum A., Kanatharana, P. Wongniramaikul, W., Daeid N. N. (2012). Rapid quantitative colourimetric tests for trinitrotoluene (TNT) in soil, Forensic Sci. Int. 222: 340-345.

Choodum, A., Daeid. N. N., (2011). Digital image-based colourimetric tests for amphetamine and methamphetamine, Drug Test. Anal. 3: 277-282.

Choodum, A., Kanatharana, P., Wongniramaikul, W., Daeid, N.N. (2013). Using the iPhone as a device for a rapid quantitative analysis of trinitrotoluene in soil, Talanta 115: 143-149.

Choodum, A., Parabun K., Klawach N., Daeid N. N., Kanatharana, P. Wongniramaikul, W. (2014). Real time quantitative colorimetric test for methamphetamine detection using digital and mobile phone technology, Forensic Sci. Int. 235: 8–13.

Christison T, De Borbra B, Rohrer J. Determination of Total Cyanide in Municipal Wastewater and Drinking Water Using Ion-Exclusion Chromatography with Pulsed Amperometric Detection (ICE-PAD). Thermo Fisher Scientific, Sunnyvale, CA.

Cura, J. A., Jansson, P. E., Krisman, C. R. (1995). Amylose is not linear. Starch/Starke, 47(6): 207-209.

Eisler, R., Clark Jr, D.R., Wiemeyer, S.N. and Henny, C.J. (1999). Sodium cyanide hazards to fish and other wildlife from gold mining operations. In Environmental Impacts of Mining Activities, pp. 55-67. Springer Berlin Heidelberg.

Epperson, P. M., Sweedler, J. V., Bilhorn, R. B., Sims, G. R. and Denton, M. B. (1988). Applications of charge transfer devices in spectroscopy. Analytical Chemistry, 60(5): 327A-335A.

Gaiao, E.D.N., Martins, V.L., Lyra, W.D.S. Almeida, L.F.D., Silva, E.C.D., Arajo, M.C.U. (2006). Digital image-based titrations. Anal. Chim. Acta, 570: 283–290.

Gale, P.A., Caltagirone, C. (2015). Anion sensing by small molecules and molecular ensembles. Chemical Society Reviews, 44(13), pp.4212-4227.

Goddijn, L.M. and White, M. (2006). Using a digital camera for water quality measurements in Galway Bay. Estuarine, coastal and shelf science, 66(3): 429-436.

Hyun, Y. J., Seul, A. L., Yu J. N., Gyeong, J. P., Cheal, K. (2015). A colorimetric Schiff base chemosensor for CN^- by naked-eye in aqueous solution. Inorganic Chemistry Communications, 54: 73-76.

Isaad, J., Achari, A. E., Malek F. (2013). Bio-polymer starch thin film sensor for low concentration detection of cyanide anions in water. Dyes and Pigment, 97: 134-140.

Isaad, J., El Achari, A., Malek, F. (2013). Bio-polymer starch thin film sensor for low concentration detection of cyanide anions in water. Dyes and pigments, 97(1), 134-140.

Jenk, W. R. (1985). Potassium Cyanide. (In) Kirk-Othmer Encyclopedia of Chemical Technology, 3rd ed., Volume 7. R. E. Kirk, et al., eds., John Wiley and Sons, New York, NY.

Jung, H. S., Han J. H., Kim Z. H., Kang C., Kim J.S. (2011) Coumarin-Cu(II) ensemble-based cyanide sensing chemodosimeter, Org. Lett. 13, 5056-5059.

Junjian Li, Xiaoliang Qi, Wei Wei, Yucheng Liu, Xiao Xu, Qiuhan Lin, Wei Dong. (2015). A “donor-two-acceptor” sensor for cyanide detection in aqueous solution. Sensors and Actuators B: Chemical, 220: 986-991.

Jun-Jian, L., Wei, W., Xiao-Liang, Q., Xiao, X., Yu-Cheng, Liu., Qiu-Han, L., Wei Dong. (2016). Rational design, synthesis of reaction-based dual-channel cyanide sensor in aqueous solution. 152: 288-293.

Kage, S., Nagata, T., & Kudo, K. (1994). Determination of cyanide in blood by GCECD and GC-MS. Japanese Journal of Forensic Toxicology, 12: 130-131.

Kaur, K., Saini, R., Kumar, A., Luxami, V., Kaur, N., Singh, P., Kumar, S. (2012) Chemodosimeters: an approach for detection and estimation of biologically and medically relevant metal ion, anions and thiols, coord. Chem. Rev. 256: 1992-2028.

Kew-Yu Chen, Wei-Chi Lin (2015). A simple 7-azaindole-based ratiometric fluorescent sensor for detection of cyanide in aqueous media. Dyes and Pigments, 123: 0143-7208.

Komatsu, K., Urano, Y., Kojima, H. and Nagano, T., (2007). Development of an iminocoumarin-based zinc sensor suitable for ratiometric fluorescence imaging of neuronal zinc. Journal of the American Chemical Society, 129(44):13447-13454.

Kompany-Zareh, M., Mansourian, M., Ravaee, F. (2002). Simple method for colourimetric spot-test quantitative analysis of Fe(III) using a computer controlled hand-scanner, Anal. Chim. Acta 471: 97–104.

Kulig, K.W., Ballantyne, B. (1991). Cyanide toxicity (Vol. 15). US Department of Health & Human Services, Public Health Service, Agency for Toxic Substances and Disease Registry.

Lakowiez, J. R. (1991). Principles. In topics in Fluorescence Spectroscopy, Plenum Press: New York. Vol 2.

Lee, J. H., Jeong A.R., Shin I.S., Kim, Hong H.J., J.I. (2010). Fluorescence turn-on sensor for cyanide based on a cobalt(II)-coumarinylsalen complex, Org. Lett. 12, 764-767.

Liu, E. (2012). The Synthesis of a New Reagent for Detecting Cyanide. Orient. J. Chem, 28(1): 19-22.

Long L, Wang L, Wu Y. (2013). A Fluorescence Ratiometric Probe for Detection of Cyanide in Water Sample and Living Cells. Advances in Materials Physics and Chemistry, 3: 307-313.

Lopez-Molinero, A., Cubero V. T., Irigoyen R. D., Piazuelo, D. S. (2013) Feasibility of digital image colourimetry—Application for water calcium hardness determination, Talanta 103, 236-244.

Lopez-Molinero, A., Linan, D., Sipiera D., Falcon, R. (2010). Chemometric interpretation of digital image colourimetry. Application for titanium determination in plastics, Microchem. J. 96: 380-385.

Lopez-Molinero, A., Linan, D., Sipiera D., Falcon, R. (2010). Chemometric interpretation of digital image colourimetry. Application for titanium determination in plastics, Microchem. J. 96, 380-385.

Lou, X., Qin, J., & Li, Z. (2009). Colorimetric cyanide detection using an azobenzene acid in aqueous solutions. Analyst, 134(10): 2071-2075.

Luo, J.D., Xie, Z., Lam, J.W., Cheng, L., Chen, H., Qiu, C., Kwok, H.S., Zhan, X., Liu, Y., Zhu, D. and Tang, B.Z. (2001). Aggregation-induced emission of 1-methyl-1, 2, 3, 4, 5-pentaphenylsilole, Chem Commun, 21(18): 1740-1741.

Martínez, M.A. and Ballesteros, S. (2006). Suicidal inhalation of motorbike exhaust: adding new data to the literature about the contribution of gasoline in the cause of death. Journal of analytical toxicology 30: 697-702.

Mathew, A.S., DeRosa, C.A., Demas, J.N. and Fraser, C.L., 2016. Difluoroboron β-diketonate materials with long-lived phosphorescence enable lifetime based oxygen imaging with a portable cost effective camera. Analytical Methods, 8(15), pp.3109-3114.

Miller JC, Miller JN. Statistic and Chemometric for Analytical Chemistry. 6th edition. Pearson Education Limited, Essex, UK. 2010.

Miller, G.C., Pritsos, C.A. (2001). Cyanide: social, industrial, and economic aspects, Proc. Symp. Annu. Meet. TMS. pp. 73–81.

Na, Y.J., Park, G.J., Jo, H.Y., Lee, S.A. and Kim, C. (2014). A colorimetric chemosensor based on a Schiff base for highly selective sensing of cyanide in aqueous solution: the influence of solvents. New Journal of Chemistry, 38(12): 5769-5776.

National Primary Drinking Water Regulation. Code of Federal Regulations, Part 141, Title 40, 2008; Fed. Regis. 2008; 22, 448.

Nicoleti, C. R., Nandi, L. G., & Machado, V. G. (2015).Chromogenic chemodosimeter for highly selective of cyanide in water and blood plasma based on si-O cleavage in the micellar system. Analytical Chemistry, 87(1): 362-366).

Noh, J.Y., Hwang, I.H., Kim, H., Song, E.J., Kim, K.B. and Kim, C. (2013). Salicylimine-based colorimetric and fluorescent chemosensor for selective detection of cyanide in aqueous buffer. Bull. Korean Chem, Soc, 34(7): 1985.

Pati, P. B. (2016). Organic chemodosimeter for cyanide: A nucleophilic approach. Sensors and Actuators B: Chemical, 222, 374–390.

Peng, L., Wang, M., Zhang, G., Zhang, D., and Zhu, D. (2009). A Fluorescence Turn-on Detection of Cyanide in Aqueous Solution Based on the Aggregation-Induced Emission, organic letters, 11(9): 1943-1946.

Persaud, K., Dodd, G. (1982). Analysis of discrimination mechanism in the mammalian olfactory system using a model nose. 352-355.

Pitschmann, V., Kobliha, Z. and Tušarová, I., (2011). A Simple Spectrophotometric Determination of Cyanides by P-nitrobenzaldehyde and Tetrazolium Blue. Advances in Military Technology, 6(2).

R. Koenig, Science (2000). Wildlife deaths are a grim wake-up call in Eastern Europe. Science 287: 1737-1738.

Raju, J., & Gupta, V. K. (1989). Spectrophotometric determination of hydrogen cyanide in air and its application in biological samples. Asian Environment, 11: 66-72.

Santos, Carla IM, Elisabete Oliveira, Joana FB Barata, M. Amparo F. Faustino, José AS Cavaleiro, M. Graça PMS Neves, and Carlos Lodeiro.(2014). "New gallium (III) corrole complexes as colorimetric probes for toxic cyanide anion." Inorganica Chimica Acta 417: 148-154.

Selkoe, D. J., & Schenk, D. (2003). Alzheimer's disease: molecular understanding predicts amyloid-based therapeutics. Annual review of pharmacology and toxicology, 43: 545-584.

Shan, Y., Wu, Q., Sun, N., Sun, Y., Cao, D., Liu, Z., Guan R., Xu, Y., Yu, X. (2017). Two indole chalcone derivatives as chemosensors for cyanide anions. Materials chemistry and physics, 186: 295-300.

Sharma, H., Kaur, N., Singh, A., Kuwar, A. and Singh, N., (2016). Optical chemosensors for water sample analysis. Journal of Materials Chemistry C, 4(23): 5154-5194.

Sharma, P., Rana, D. S., Umar, A., Kumar, R., Chauhan, M. S., & Chauhan, S. (2016). Hexagonal cadmium oxide nanodisks: Efficient scaffold for cyanide ion sensing and photo-catalytic applications. Talanta, 153: 57-65.

Simeonoya, P., Fishbein, L. (2004). Hydrogen cyanide and cyanide: Human Health Aspects, Concise International Chemical Assessment Document 61, Executive Summary section; Jointly by United Nations Environment Program, International Labor Organization, and World Health Organization, within the Inter-Organization Program for sound Management of chemicals: Geneva, 10-11

Srikun, D., Miller, E.W., Domaille, D.W. and Chang, C.J. (2008). An ICT-based approach to ratiometric fluorescence imaging of hydrogen peroxide produced in living cells. Journal of the American Chemical Society, 130(14): 4596-4597.

Suzuki, Y., Endo, M., Jin, J., Iwase, K., Iwatsuki, M. (2006). Tristimulus Colourimetry Using a Digital Still Camera and Its Application to Determination of Iron and Residual Chlorine in Water Samples, Anal. Sci. 22(3), 411-414.

Thongprajukaew K., Choodum, A., Sa-E, B and Hayee, U. (2014). Smart phone: A popular devise support amylase assay in fisheries research. Food Chemistry, 163, 87-91.

Tivana, L. D., Francisco, J. D. C., Zelder, F., Bergenstahl, B and Dejmek, P. (2014). Straightforward rapid spectrophotometric quantification of total cyanogenic glycosides in fresh and processed cassava product, Food Chemistry, 158: 20-27.

Tomasulo, M., Françisco M. R. (2005) "Colorimetric detection of cyanide with a chromogenic oxazine." Organic letters 7(21): 4633-4636.

Tong, H., Hong, Y., Dong, Y., Häussler, M., Li, Z., Lam, J.W., Dong, Y., Sung, H.H.Y., Williams, I.D. and Tang, B.Z. (2007). Protein detection and quantitation by tetraphenylethene-based fluorescent probes with aggregation-induced emission characteristics. The Journal of Physical Chemistry B, 111(40): 11817-11823.

Tremblay MS., Halim M, Sames D. (2007). Cocktails of Tb^{3+} and Eu^{3+} complexes: a general platform for the design of ratiometric optical probes. J Am Chem Soc, 129: 7570-7.

Vennesland, B., Comm E. E., Knownles, C. J., Westly, J. and Wissing, F. (1981). Cyanide in biology, Academic Press, London.

Water Quality Standards. Code of Federal Regulations, *Part* 131, Title 40, 2008; Fed. Regist.2008; 21: 451–463.

Weinberg, H. S.; Cook, S. J. (2002). Segmented flow injection, UV digestion, and amperometric detection for the determination of total cyanide in wastewater treatment plant effluents, Anal. Chem, 74 (23): 6055–6063.

Wu, W., Tang, R., Li, Q., & Li, Z. (2015). Functional hyperbranched polymer with advanced optical, electrical and magnetic properties. Chemical Society Reviews, 44(12), 3997-4022

Xu, Z., Chen, X., Kim, H. N., & Yoon, J. (2010). Sensors for the optical detection of cyanide ion. Chemical Society Reviews, 39(1): 127-137.

Yuning, H., Jacky, W.Y.L., Ben T. (2009). Aggregation induced emission: phenomenon, mechanism and applications. Chemical communication, 4332-4353.

Zhang P, Shi BB, Wei TB, Zhang YM, Lin Q, Yao H. (2013). A naphtholic Schiff base for highly selective sensing of cyanide via different channels in aqueous solutions. Dyes Pigments, 99: 857-62.

Zheng Wei. (2011). Research progresses in bio-treatment of wastewater containing cyanide Environmental Protection of Chemical Industry 31: 123-128.

Vitae

Name Mr. Doe-Puplampu Seth

Student ID 5830222002

Educational Attainment:

Degree	Name of Institution	Year
Bachelor of Science (Materials Engineering)	Kwame Nkrumah University Of Science and Technology	2013

Scholarship Awards during Enrolment

Best Student Poster Presentation at the 27th Annual International Conference on Soil, Water, Energy and Air. March 20-23, 2017, San Diego, CA, USA.

Faculty of Technology and Environment scholarship, Prince of Songkla University, 2015, Phuket-Thailand.

Applied Chemistry and Environmental Technology Research Center (ACET-RC) Scholarship, 2015, PSU-Phuket, Thailand.

List of Publications and Proceeding

AEHS 2017, “Detection of Cyanide in Water by Environmentally Friendly Calorimetry with Digital Image Analysis”. San Diego, CA, USA.

PACCON 2017, “Detection of Cyanide in Water by Environmentally Friendly Calorimetry with Digital Image Analysis”. Bangkok, Thailand.